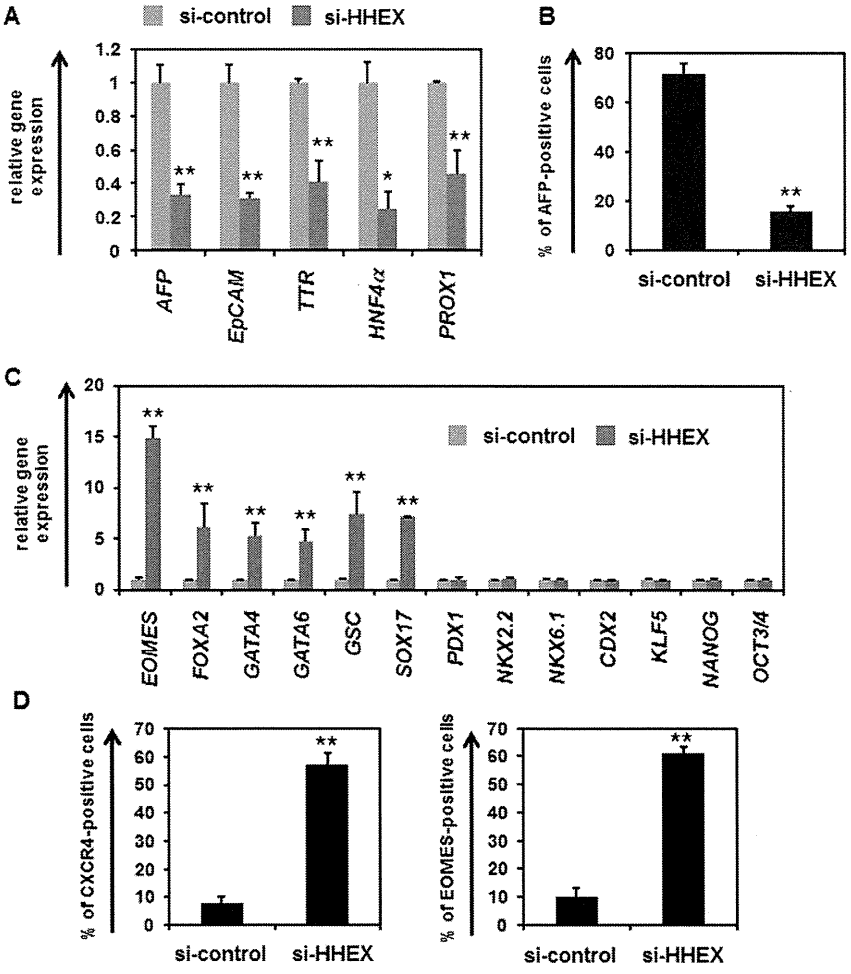

Figure 1. The expression levels of DE markers in the si-HHEX-transfected cells were upregulated in hepatoblast differentiation from DE cells. (**A**) hESCs (H9) were differentiated into DE cells according to the protocol described in the *Materials and Methods* section. The DE cells were transfected with 50 nM si-control or si-HHEX on day 4, and cultured in the medium containing 20 ng/ml BMP4 and 20 ng/ml FGF4 until day 9. On day 9, the gene expression levels of hepatoblast markers (*AFP*, *EpCAM*, *TTR*, *HNF4α*, and *PROX1*) in si-control- or si-HHEX-transfected cells were examined by real-time RT-PCR. The gene expression levels in the si-control-transfected cells were taken as 1.0. (**B**) On day 9, the percentage of AFP-positive cells was measured by using FACS analysis to examine the hepatoblast differentiation efficiency. (**C**) The gene expression levels of DE (*EOMES*, *FOXA2*, *GATA4*, *GATA6*, *GSC*, and *SOX17*), pancreatic (*PDX1*, *NKX2.2*, and *NKX6.1*), intestinal (*CDX2* and *KLF5*), and pluripotent markers (*NANOG* and *OCT3/4*) in the si-control- or si-HHEX-transfected cells were examined by real-time RT-PCR. The gene expression levels in the si-control-transfected cells were taken as 1.0. (**D**) On day 9, the percentage of cells positive for the DE markers (CXCR4 and EOMES) was examined by using FACS analysis. All data are represented as means ± SD ($n = 3$). *$p<0.05$, **$p<0.01$.
doi:10.1371/journal.pone.0090791.g001

Each 5′ UTR of the human EOMES was cloned into the promoter region of the pGL3-Basic vector (Promega) using KpnI and NcoI restriction sites. In addition, the 400 bp region around the HHEX response element (HRE) was amplified by using the following primers: 5′-CCTGCTAGCGTTCTCTGG-TACTTTTCAAAATGGTGC-3′ and 5′-GAAAACTAG-TATGCGCCTGTGCAAGGGAATAGAATCAG-3′. The 400 bp region around the HRE was cloned into the enhancer region of each of pGL3-EOM-5UTR1000 and pGL3-EOM-5UTR4000 using XbaI restriction site to generate pGL3-EOM-5UTR1000 containing the region around the HRE (p5′ EOM-Luc) and pGL3-EOM-5UTR4000 containing the region around the HRE (pLong-5′ EOM-Luc).

To generate pGL3-EOM-5UTR1000 containing the region which has a mutated HRE reporter construct (p5′ EOM-mut-Luc), the following base substitutions were introduced into the 400 bp region around the HRE: 5′-TCCCAATTAAAATC-3′ to 5′-TCC***AGC***T***G***A***C***AATC-3′. PCR products were cloned into the enhancer region of pGL3-EOM-5UTR1000 using XbaI restriction site.

Luciferase Reporter Assays

HeLa cells were transfected with each of the firefly luciferase reporter plasmids described above (p5′ EOM-Luc or p5′ EOM-mut-Luc) or control plasmids, pGL3-Basic vector plasmids (pControl-Luc), by using Lipofectamine 2000 (Invitrogen)-mediated gene transfection according to the manufacturer's instructions. HeLa cells were seeded at a density of 2.0×10^5 cells/well in 24-well tissue culture plates, and cultured for 24 hours before transfection. HeLa cells were transfected with 333 ng/well of each firefly luciferase reporter plasmids (pControl-Luc, p5′ EOM-Luc, or p5′ EOM-mut-Luc), 333 ng/well of HHEX expression plasmids (pHMEF5-HHEX [13]) or blank expression plasmids (pHMEF5), and 333 ng/well of internal control plasmids (pCMV-

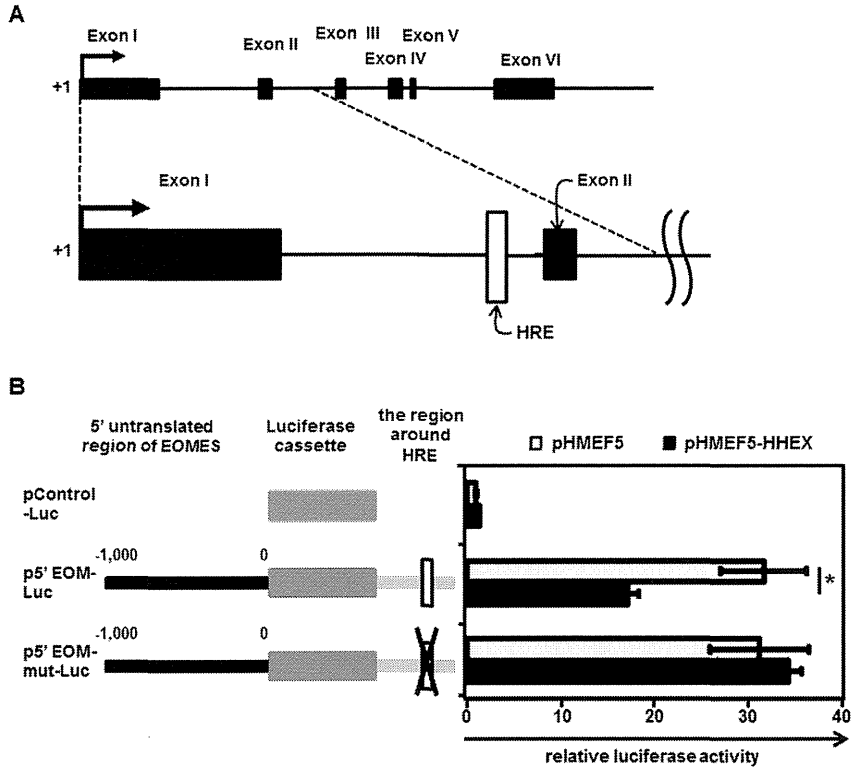

Figure 2. HHEX suppresses EOMES expression by binding to the HRE located in the first intron of EOMES. (**A**) An overview of the EOMES mRNA precursor and the location of the putative HRE are presented. The HRE is located in the first intron of EOMES. (**B**) Luciferase reporter assays were performed to examine the regulation of EOMES expression by HHEX. HeLa cells were cotransfected with both firefly luciferase reporter plasmids (pControl-Luc, p5′ EOM-Luc, or p5′ EOM-mut-Luc) and effecter plasmids (control plasmids (pHMEF5) or HHEX expression plasmids (pHMEF5-HHEX)). The details of the luciferase reporter assays are described in the *Materials and Methods* section. The luciferase activities in the pControl-Luc- and pHMEF5-cotransfected cells were taken as 1.0. All data are represented as means ± SD ($n=3$). *, $p<0.05$.
doi:10.1371/journal.pone.0090791.g002

Renilla luciferase), and cultured for 72 hours. The luciferase activities in the cells were measured by using Dual Luciferase Assay System (Promega) according to the manufacturer's instructions. Firefly luciferase activities in the cells were normalized by the measurement of renilla luciferase activities. The luciferase activity in the cells cotrasfected with pControl-Luc and pHMEF5 was assigned a value of 1.0.

siRNA Transfection

Knockdown of HHEX or EOMES was performed using a specific small interfering RNA (siRNA) fourplex set targeted to HHEX or EOMES, respectively (Darmacon SMARTpool) (Thermo Fisher Scientific). Si-Control (Darmacon siGENOME Non-Targeting siRNA Pool) (Thermo Fisher Scientific) was used as a control. Lipofectamine RNAiMAX (Invitrogen)-mediated gene transfection was used for the reverse transfection according to the manufacturer's instructions. The hESC-derived DE cells on day 4 were transfected with 50 nM of siRNA for 6 hours by reverse transfection.

Immunohistochemistry

The hESC-derived cells were fixed with methanol or 4% PFA. After blocking with PBS containing 1% BSA (Sigma), 0.2% Triton X-100 (Sigma), and 10% FBS, the cells were incubated with primary antibody at 4°C overnight, followed by incubation with a secondary antibody that was labeled with Alexa Fluor 488 (Invitrogen) at room temperature for 1 hour. All the antibodies are listed in **Table S2 in File S2**.

Western Blotting Analysis

The hESC-derived cells were homogenized with lysis buffer (20 mM HEPES, 2 mM EDTA, 10% glycerol, 0.1% SDS, 1% sodium deoxycholate, and 1% Triton X-100) containing a protease inhibitor mixture (Sigma). After being frozen and thawed, the homogenates were centrifuged at 15,000 *g* at 4°C for 10 minutes, and the supernatants were collected. The lysates were subjected to SDS-PAGE on 7.5% polyacrylamide gel and were then transferred onto polyvinylidene fluoride membranes (Millipore). After the reaction was blocked with 1% skim milk in TBS containing 0.1% Tween 20 at room temperature for 1 hour, the membranes were incubated with anti-human HHEX, EOMES, or β-actin antibodies at 4°C overnight, followed by reaction with horseradish peroxidaseconjugated anti-rabbit IgG or anti-mouse IgG antibodies at room temperature for 1 hour. The band was visualized by ECL Plus Western blotting detection reagents (GE Healthcare) and the signals were read using an LAS-4000 imaging system (Fuji Film). All the antibodies are listed in **Table S2 in File S2**.

Results

Obstruction of Hepatoblast Differentiation by HHEX Knockdown Results in Upregulation of the Expression Levels of DE Markers

It is known that HHEX plays an important role in hepatoblast differentiation [11–12–14]. We have previously reported that HHEX overexpression promoted hepatoblast differentiation from

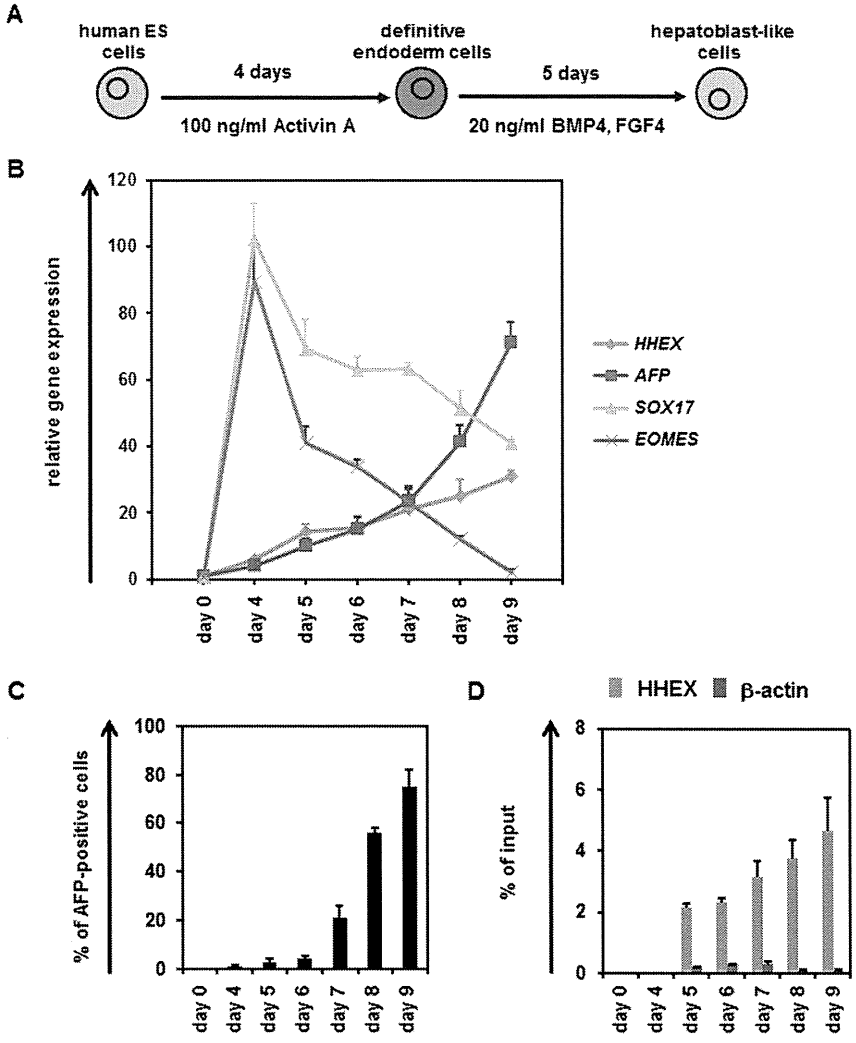

Figure 3. Temporal analysis of endogenous gene expression levels of EOMES and HHEX in hepatoblast differentiation from hESCs. (**A**) The schematic protocol for hepatoblast differentiation from hESCs (H9) is shown. (**B**) The temporal gene expression levels of *HHEX, AFP, SOX17* and *EOMES* were examined by real-time RT-PCR in hepatoblast differentiation. The gene expression levels in undifferentiated hESCs were taken as 1.0. (**C**) To examine the hepatoblast differentiation efficiency, the percentage of AFP-positive cells was measured by FACS analysis. (**D**) The HHEX protein-binding frequencies of the regions around the HRE of the EOMES gene and a negative control gene (β-ACTIN) were measured by ChIP-qPCR analysis. The results are presented as the percent input of anti-HHEX samples compared with those of anti-IgG samples. All data are represented as means ± SD ($n = 3$).

doi:10.1371/journal.pone.0090791.g003

the hESC-derived DE cells [13]. To confirm the importance of HHEX in hepatoblast differentiation, a loss of function assay of HHEX was performed by using siRNA-mediated HHEX knockdown. We confirmed the knockdown of HHEX expression in the hESC-derived DE cells that has been transfected with si-HHEX (**Fig. S1 in File S1**). The gene expression levels of hepatoblast markers in the si-HHEX-transfected cells were significantly downregulated as compared with those in the si-control-transfected cells (**Fig. 1A**). In addition, the percentage of alpha-fetoprotein (AFP; a hepatoblast marker)-positive cells was decreased by HHEX knockdown on day 9 (**Fig. 1B**). These results suggest that hepatoblast differentiation is prevented by HHEX knockdown, demonstrating that HHEX plays an important role in hepatoblast differentiation from DE cells. To characterize the si-HHEX-transfected cells on day 9, the gene expression levels of DE, pancreatic, intestinal, and pluripotent markers were examined (**Fig. 1C**). Interestingly, the gene expression levels of DE markers were significantly upregulated by HHEX knockdown, although those of pancreatic, intestinal, and pluripotent markers were not changed by HHEX knockdown. Furthermore, the percentage of DE marker (CXCR4 and EOMES)-positive cells was increased by HHEX knockdown (**Fig. 1D**). In addition, the percentage of AFP-positive cells or *EOMES* expression level was decreased or increased, respectively, by HHEX knockdown not only in the DE cells (day 4) but also in the cells starting to commit to hepatoblast (day 5–7) (**Fig. S2 in File S1**). This suggested that HHEX knockdown inhibits hepatoblast differentiation but does not simply change the number of the DE cells. These results suggest that the inhibition of HHEX expression during hepatoblast differentiation results in an increase of DE cells, but not pancreatic, intestinal, or undifferentiated cells.

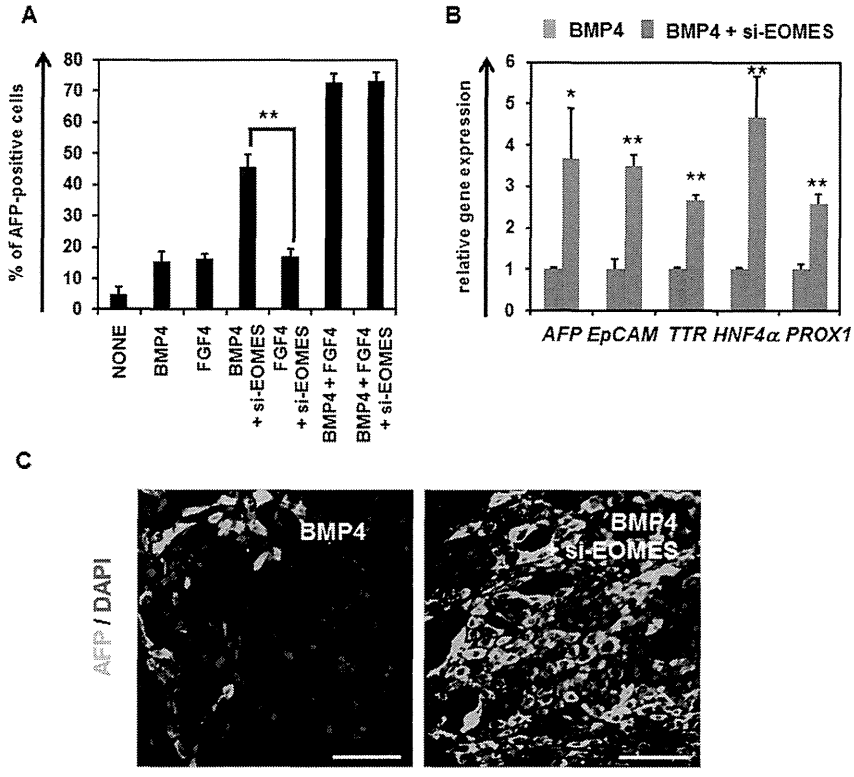

Figure 4. Hepatoblast differentiation was promoted by knockdown of EOMES in the presence of BMP4. (**A**) The hESCs (H9) were differentiated into the DE cells according to the protocol described in the *Materials and Methods* section. The hESC-derived DE cells were transfected with 50 nM si-control or si-EOMES on day 4, and then cultured with the medium containing BMP4 or FGF4. The percentage of AFP-positive cells was examined by FACS analysis on day 9. (**B**) The gene expression levels of hepatoblast markers (*AFP*, *EpCAM*, *TTR*, *HNF4α*, and *PROX1*) were measured by real-time RT-PCR on day 9. The gene expression levels in si-control-transfected cells were taken as 1.0. (**C**) The si-control- or si-EOMES-transfected cells were subjected to immunostaining with anti-AFP (green) antibodies. Nuclei were counterstained with DAPI (blue). The bar represents 50 μm. All data are represented as means ± SD ($n=3$). *$p<0.05$, **$p<0.01$.
doi:10.1371/journal.pone.0090791.g004

HHEX Directly Represses EOMES Expression

Because the gene expression level of *EOMES* was most increased by HHEX knockdown in hepatoblast differentiation, we expected that EOMES might be directly regulated by HHEX. The putative HHEX-binding site (HHEX response element (HRE)) [22] was found in the first intron of EOMES as shown in **Figure 2A**. To investigate whether HHEX could directly repress EOMES transcription, luciferase reporter assays were performed. The reporter plasmids that contain a 5′ untranslated region (UTR) of EOMES (**Fig. S3 in File S1**) and the first intron of EOMES were generated because the putative HHEX-binding site was observed in the first intron of EOMES. The luciferase reporter assays showed that p5' EOM-Luc, which contains the wild-type HRE, mediates significant repression of luciferase activity by HHEX overexpression, whereas p5' EOM-mut-Luc, which contains a mutant HRE, mediates similar luciferase activity even in the presence of HHEX (**Fig. 2B**). These results indicated that HHEX represses EOMES expression through the HRE located in the first intron of EOMES.

Endogenous Temporal Gene Expression Analysis of HHEX and EOMES in Hepatic Specification

To examine the relationship between HHEX and EOMES in hepatic specification, the temporal gene expression patterns of *HHEX* and *EOMES* were examined in hepatoblast differentiation from hESCs (**Fig. 3A**). In DE differentiation (from day 0 to 4), the gene expression levels of *EOMES* and *SOX17* were increased, although those of *HHEX* and *AFP* did not change (**Fig. 3B**). In the hepatic specification process (from day 5 to 9), the gene expression levels of *HHEX* and *AFP* began to be upregulated on day 5, and continued to increase until day 9. On the other hand, the gene expression levels of *EOMES* and *SOX17* started to decrease on day 5, and continued to decrease until day 9. We confirmed that the percentage of CXCR4-positive cells was 95.2±2.2% on day4. In addition, we confirmed that few AFP-positive cells were observed on day 5, and that the percentage of AFP-positive cells continuously increased until day 9 (**Fig. 3C**). To examine whether HHEX binds to the HRE located in the first intron of EOMES, ChIP-qPCR analysis of hepatoblast differentiation from hESCs was performed (**Fig. 3D**). HHEX bound to the HRE located in the first intron of EOMES on day 5, when the hepatic specification began. The amount of HHEX binding to that site continued to increase until day 9. These results suggest that HHEX binds to HRE located in the first intron of EOMES in hepatic specification from the DE cells.

EOMES Knockdown Promotes Hepatic Specification in the Presence of BMP4

To examine the function of EOMES in hepatoblast differentiation, EOMES was knocked down in the DE cells in the presence of BMP4 or FGF4. We confirmed the knockdown of EOMES expression in the hESC-derived DE cells that has been transfected with si-EOMES (**Fig. S4 in File S1**). Although the percentage of AFP-positive cells was increased by EOMES knockdown in the

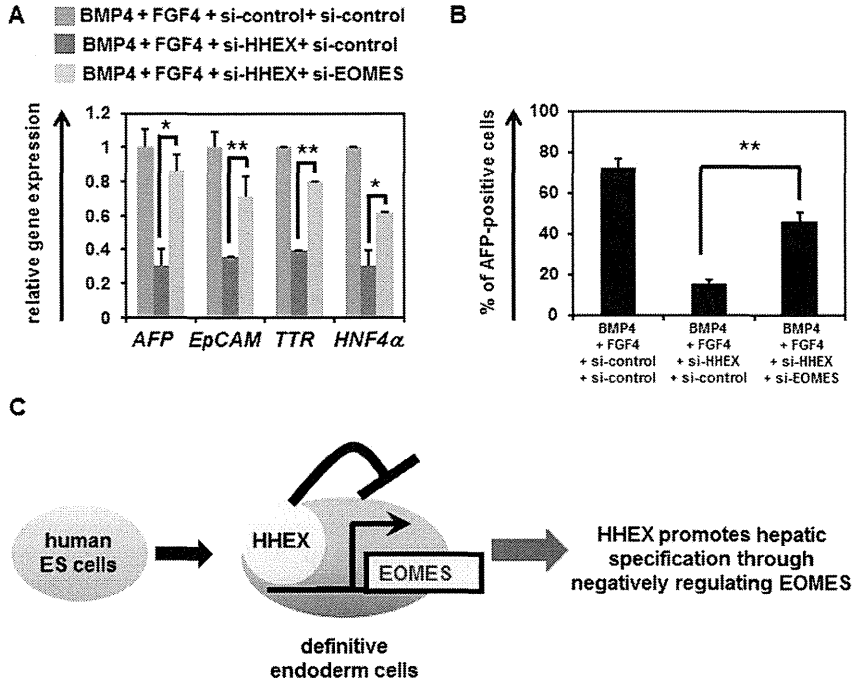

Figure 5. Hepatoblast differentiation is inhibited by EOMES, which functions downstream of HHEX. (**A**) The hESCs (H9) were differentiated into the DE cells according to the protocol described in the *Materials and Methods* section. The hESC-derived DE cells were transfected with 50 nM si-control, si-EOMES, or si-HHEX on day 4, and then cultured with the medium containing BMP4 and FGF4. The gene expression levels of hepatoblast markers (*AFP*, *EpCAM*, *TTR*, and *HNF4α*) were measured by real-time RT-PCR on day 9. The gene expression levels in si-control- and si-HHEX-transfected cells were taken as 1.0. (**B**) The percentage of AFP-positive cells was examined by FACS analysis on day 9. All data are represented as means ± SD ($n=3$). *$p<0.05$, **$p<0.01$. (**C**) HHEX promotes the hepatic specification from the hESC-derived DE cells by negatively regulating EOMES expression. A model of the hepatic specification from the hESC-derived DE cells by HHEX is presented. In the hESC-derived DE cells, HHEX represses EOMES expression. In this way, HHEX promotes the hepatic specification from the hESC-derived DE cells.
doi:10.1371/journal.pone.0090791.g005

presence of BMP4, it was not changed by EOMES knockdown in the presence of FGF4 (**Fig. 4A**). In addition, EOMES knockdown did not affect the percentage of AFP-positive cells in the presence of both FGF4 and BMP4. This might have been because the endogenous *EOMES* expression level was already sufficiently suppressed under the existence of FGF4 (**Fig. S5 in File S1**). To further investigate the function of EOMES in hepatoblast differentiation, gene expression and immunohistochemical analyses of hepatoblast markers were performed in si-EOMES-transfected cells. The gene expression levels of hepatoblast markers in si-EOMES-transfected cells were upregulated as compared with those in si-control-transfected cells (**Fig. 4B**). Consistently, the immunohistochemical analysis of AFP showed that EOMES knockdown upregulated the expression levels of AFP (**Fig. 4C**). In addition, EOMES knockdown increased the percentage of AFP-positive cells not only in the DE cells (day 4) but also in the cells starting to commit to hepatoblast (day 5–7) (**Fig. S6 in File S1**). This suggested that EOMES knockdown promotes hepatoblast differentiation but does not simply change the number of the DE cells. These results suggest that hepatic specification from the DE cells is promoted by EOMES knockdown depending on the existence of BMP4.

EOMES Functions Downstream of HHEX in the Hepatic Specification from the DE Cells

To examine whether EOMES functions downstream of HHEX in the hepatic specification from the DE cells, both HHEX and EOMES were knocked down in the DE cells, and then the gene expression profiles of hepatoblast markers were analyzed. The gene expression levels of hepatoblast markers were upregulated in both si-HHEX- and si-EOMES-transfected cells as compared with those in si-HHEX-transfected cells (**Fig. 5A**). Furthermore, the percentage of AFP-positive cells was also increased by double-knockdown of HHEX and EOMES (**Fig. 5B**). These results suggest that EOMES knockdown could promote the hepatic specification from the DE cells by HHEX knockdown. In conclusion, EOMES exerts downstream of HHEX in the hepatic specification from the DE cells.

Discussion

The purpose of this study was to identify and characterize the target genes of HHEX in hepatic specification from DE to elucidate the functions of HHEX in this process. We clearly demonstrated that the expression of EOMES is directly suppressed by HHEX, and that EOMES is one of the crucial target genes of HHEX in the hepatic specification from the hESC-derived DE cells. We also showed that EOMES knockdown in the hESC-derived DE cells could rescue the si-HHEX-mediated inhibition of hepatic specification. Our findings indicate that promotion of the hepatic specification by HHEX in the hESC-derived DE cells would be mainly mediated by the repression of EOMES expression (**Fig. 5C**).

To explore direct target genes of HHEX in the hepatic specification, EOMES knockdown experiments were conducted (**Fig. 1**). The luciferase reporter assays (**Fig. 2B**) and ChIP-qPCR (**Fig. 3C**) indicated that HHEX represses EOMES expression by binding to the first intron of EOMES containing a putative HRE. It might be expected that HHEX recruits co-repressor proteins to

repress EOMES expression because HHEX could negatively regulate the expressions of target genes such as *vascular endothelial growth factor (Vegf)* and *vascular endothelial growth factor receptor-1 (Vegfr-1)* by forming the co-repressor protein complexes [23–25]. Previous studies demonstrated that HHEX has three main domains, a repression domain, a DNA-binding domain, and an activation domain [26], and thus exerts both positive and negative effects on the target gene expressions. Taken together, these findings suggested that HHEX would repress EOMES expression through the function of its repression domain.

The results in **figure 4A** demonstrate that EOMES knockdown promoted hepatic specification in the presence of BMP4, but not FGF4. Because it was previously reported that FGF4 could induce the expression level of HHEX in the DE cells [27], FGF4 treatment in the DE cells would lead to downregulation of EOMES expression via the regulation of HHEX expression. Therefore, HHEX and EOMES might exert in the downstream of FGF4 in the hepatic specification. In addition, both BMP4 and FGF4 are necessary for hepatic specification (**Fig. 4A**). However, the functions of BMP4 in hepatic specification and the synergistic effect of BMP and FGF have not been sufficiently elucidated, and will need to be resolved in future studies.

Simultaneous knockdown of HHEX and EOMES in the hESC-derived DE cells led to rescue of the HHEX-mediated inhibition of the hepatic specification (**Fig. 5**). These results suggested that the majority of functions in the hepatic specification by HHEX may be caused by the repression of EOMES expression. EOMES is known to regulate numerous target genes related to DE differentiation, and thus the repression of EOMES expression might also promote other DE-derived lineage specifications, such as pancreatic specification. HHEX is known to regulate not only hepatic specification but also pancreatic specification [11–28]. Therefore, EOMES might also be a target gene of HHEX in pancreatic specification as well as in hepatic specification. Because the HHEX protein is known to interact with the HNF1α protein and synergistically upregulate the HNF1α target gene expression [15], it would be of interest to examine the relationship between HHEX and HNF1α in the hepatic specification from the hESC-derived DE cells. The proteomic analyses of HHEX protein in the hepatic specification from the hESC-derived DE cells might help to elucidate the functions of HHEX in this process.

Conclusions

In summary, we showed that the homeobox gene HHEX promotes the hepatic-lineage specification from the hESC-derived DE cells through the repression of EOMES expression. Previously, we reported that transduction of SOX17, HNF4α, FOXA2 or HNF1α into the hESC-derived cells could promote efficient hepatic differentiation [16–18]. The direct target genes of these genes might be identified by using the strategy described here. Furthermore, identification of the genes targeted by functional genes in the various lineage differentiation models from hESCs will promote understanding of the intricate transcriptional networks that regulate human development.

Supporting Information

File S1 Contains the following files: **Figure S1. Knockdown of HHEX in the DE cells by si-HHEX transfection. (A, B)** The hESCs (H9) were differentiated into the DE cells (day 4) according to the protocol described in *Materials and Methods* section. The DE cells were transfected with 50 nM si-control or si-HHEX on day 4. On day 6, the HHEX expression levels in si-control- or si-HHEX-transfected cells were examined by real-time RT-PCR (**A**) or Western blotting (**B**). The gene expression levels of *HHEX* in the si-control-transfected cells were taken as 1.0. All data are represented as means ± SD ($n = 3$). ** $p<0.01$. **Figure S2. The percentage of AFP-positive cells or *EOMES* expression level was decreased or increased, respectively, by HHEX knockdown. (A, B)** The hESCs (H9) were differentiated into the DE cells according to the protocol described in the *Materials and Methods* section. The DE cells were transfected with 50 nM si-control or si-HHEX on day 4, 5, 6, or 7, and cultured in medium containing 20 ng/ml BMP4 and 20 ng/ml FGF4 until day 9. On day 9, the percentage of AFP-positive cells was measured by using FACS analysis to examine the hepatoblast differentiation efficiency (**A**). Also on day 9, the gene expression levels of EOMES in si-control- or si-HHEX-transfected cells were examined by real-time RT-PCR (**B**). The gene expression levels in the si-control-transfected cells were taken as 1.0. All data are represented as means ± SD ($n = 3$). **$p<0.01$. **Figure S3. Both 1,000 bp and 4,000 bp 5′ UTR of EOMES have promoter activities.** Luciferase reporter assays were performed to examine whether 1,000 bp and 4,000 bp 5′ UTR of EOMES have promoter activity. HeLa cells were cotransfected with both 500 ng/well of firefly luciferase reporter plasmids (pControl-Luc, p5′ EOM-Luc, or pLong-5′ EOM-Luc), and 500 ng/well of internal control plasmids (pCMV-Renilla luciferase), and cultured for 72 hours. The luciferase activities in the cells were measured by using Dual Luciferase Assay System (Promega) according to the manufacturer's instructions. Firefly luciferase activities in the cells were normalized by the measurement of renilla luciferase activities. The RLU in the pControl-Luc-transfected cells was assigned a value of 1.0. All data are represented as means ± SD ($n = 3$). *, $p<0.05$. **Figure S4. Knockdown of EOMES in the DE cells by si-EOMES transfection. (A, B)** The hESCs (H9) were differentiated into the DE cells (day 4) according to the protocol described in *Materials and Methods* section. The DE cells were transfected with 50 nM si-control or si-EOMES on day 4. On day 6, the EOMES expression levels in si-control- or si-EOMES-transfected cells were examined by real-time RT-PCR (**A**) or Western blotting (**B**). The gene expression levels of *EOMES* in the si-control-transfected cells were taken as 1.0. All data are represented as means ± SD ($n = 3$). ** $p<0.01$. **Figure S5. Hepatoblast differentiation was promoted by knockdown of EOMES.** The hESCs (H9) were differentiated into the DE cells according to the protocol described in the *Materials and Methods* section. The hESC-derived DE cells were transfected with 50 nM si-control or si-EOMES on day 4, 5, 6, or 7, and then cultured in medium containing BMP4 or FGF4. The percentage of AFP-positive cells was examined by FACS analysis on day 9. All data are represented as means ± SD ($n = 3$). **$p<0.01$. **Figure S6. The *EOMES* or *HHEX* expression level was suppressed or increased, respectively, in the presence of FGF4.** The hESCs (H9) were differentiated into the DE cells according to the protocol described in the *Materials and Methods* section. The hESC-derived DE cells were cultured in medium containing BMP4 or FGF4 until day 9. The gene expression levels of *EOMES*, *HHEX*, or *AFP* in the non-treated cells (control) were taken as 1.0. All data are represented as means ± SD ($n = 3$). **$p<$ 0.01 (compared with control).
(PDF)

File S2 Contains the following files: **Table S1.** List of primers used in this study. **Table S2.** List of antibodies used in this study.
(DOC)

Acknowledgments

We thank Yasuko Hagihara, Misae Nishijima, Nobue Hirata, and Reiko Hirabayashi for their excellent technical support.

Author Contributions

Conceived and designed the experiments: HW K. Takayama MI MT K. Katayama K. Kawabata HM. Performed the experiments: HW K. Takayama MI NM. Analyzed the data: HW K. Takayama MI MT K. Katayama K. Tashiro YN FS K. Kawabata MKF HM. Wrote the paper: HW K. Takayama HM. Contributed equally to this work: HW K. Takayama.

References

1. Zaret KS, Grompe M (2008) Generation and regeneration of cells of the liver and pancreas. Science 322: 1490–1494.
2. Si-Tayeb K, Lemaigre FP, Duncan SA (2010) Organogenesis and development of the liver. Dev Cell 18: 175–189.
3. Thomson JA, Itskovitz-Eldor J, Shapiro SS, Waknitz MA, Swiergiel JJ, et al. (1998) Embryonic stem cell lines derived from human blastocysts. Science 282: 1145–1147.
4. D'Amour KA, Agulnick AD, Eliazer S, Kelly OG, Kroon E, et al. (2005) Efficient differentiation of human embryonic stem cells to definitive endoderm. Nat Biotechnol 23: 1534–1541.
5. D'Amour KA, Bang AG, Eliazer S, Kelly OG, Agulnick AD, et al. (2006) Production of pancreatic hormone-expressing endocrine cells from human embryonic stem cells. Nat Biotechnol 24: 1392–1401.
6. Si-Tayeb K, Noto FK, Nagaoka M, Li J, Battle MA, et al. (2010) Highly efficient generation of human hepatocyte-like cells from induced pluripotent stem cells. Hepatology 51: 297–305.
7. Spence JR, Mayhew CN, Rankin SA, Kuhar MF, Vallance JE, et al. (2011) Directed differentiation of human pluripotent stem cells into intestinal tissue in vitro. Nature 470: 105–109.
8. Agarwal S, Holton KL, Lanza R (2008) Efficient differentiation of functional hepatocytes from human embryonic stem cells. Stem Cells 26: 1117–1127.
9. Takayama K, Kawabata K, Nagamoto Y, Inamura M, Ohashi K, et al. (2014) CCAAT/enhancer binding protein-mediated regulation of TGFbeta receptor 2 expression determines the hepatoblast fate decision. Development 141: 91–100.
10. Bogue CW, Ganea GR, Sturm E, Ianucci R, Jacobs HC (2000) Hex expression suggests a role in the development and function of organs derived from foregut endoderm. Dev Dyn 219: 84–89.
11. Bort R, Signore M, Tremblay K, Martinez Barbera JP, Zaret KS (2006) Hex homeobox gene controls the transition of the endoderm to a pseudostratified, cell emergent epithelium for liver bud development. Dev Biol 290: 44–56.
12. Keng VW, Yagi H, Ikawa M, Nagano T, Myint Z, et al. (2000) Homeobox gene Hex is essential for onset of mouse embryonic liver development and differentiation of the monocyte lineage. Biochem Biophys Res Commun 276: 1155–1161.
13. Inamura M, Kawabata K, Takayama K, Tashiro K, Sakurai F, et al. (2011) Efficient Generation of Hepatoblasts From Human ES Cells and iPS Cells by Transient Overexpression of Homeobox Gene HEX. Mol Ther 19: 400–407.
14. Kubo A, Kim YH, Irion S, Kasuda S, Takeuchi M, et al. (2010) The homeobox gene Hex regulates hepatocyte differentiation from embryonic stem cell-derived endoderm. Hepatology 51: 633–641.
15. Tanaka H, Yamamoto T, Ban T, Satoh S, Tanaka T, et al. (2005) Hex stimulates the hepatocyte nuclear factor 1alpha-mediated activation of transcription. Arch Biochem Biophys 442: 117–124.
16. Takayama K, Inamura M, Kawabata K, Tashiro K, Katayama K, et al. (2011) Efficient and Directive Generation of Two Distinct Endoderm Lineages from Human ESCs and iPSCs by Differentiation Stage-Specific SOX17 Transduction. PLoS One 6: e21780.
17. Takayama K, Inamura M, Kawabata K, Katayama K, Higuchi M, et al. (2012) Efficient Generation of Functional Hepatocytes From Human Embryonic Stem Cells and Induced Pluripotent Stem Cells by HNF4alpha Transduction. Mol Ther 20: 127–137.
18. Takayama K, Inamura M, Kawabata K, Sugawara M, Kikuchi K, et al. (2012) Generation of metabolically functioning hepatocytes from human pluripotent stem cells by FOXA2 and HNF1alpha transduction. J Hepatol 57: 628–636.
19. Takayama K, Kawabata K, Nagamoto Y, Kishimoto K, Tashiro K, et al. (2013) 3D spheroid culture of hESC/hiPSC-derived hepatocyte-like cells for drug toxicity testing. Biomaterials 34: 1781–1789.
20. Nagamoto Y, Tashiro K, Takayama K, Ohashi K, Kawabata K, et al. (2012) The promotion of hepatic maturation of human pluripotent stem cells in 3D co-culture using type I collagen and Swiss 3T3 cell sheets. Biomaterials 33: 4526–4534.
21. Takayama K, Nagamoto Y, Mimura N, Tashiro K, Sakurai F, et al. (2013) Long-Term Self-Renewal of Human ES/iPS-Derived Hepatoblast-like Cells on Human Laminin 111-Coated Dishes. Stem Cell Reports 1: 322–335.
22. Cong R, Jiang X, Wilson CM, Hunter MP, Vasavada H, et al. (2006) Hhex is a direct repressor of endothelial cell-specific molecule 1 (ESM-1). Biochem Biophys Res Commun 346: 535–545.
23. Noy P, Williams H, Sawasdichai A, Gaston K, Jayaraman PS (2010) PRH/Hhex controls cell survival through coordinate transcriptional regulation of vascular endothelial growth factor signaling. Mol Cell Biol 30: 2120–2134.
24. Guiral M, Bess K, Goodwin G, Jayaraman PS (2001) PRH represses transcription in hematopoietic cells by at least two independent mechanisms. J Biol Chem 276: 2961–2970.
25. Swingler TE, Bess KL, Yao J, Stifani S, Jayaraman PS (2004) The proline-rich homeodomain protein recruits members of the Groucho/Transducin-like enhancer of split protein family to co-repress transcription in hematopoietic cells. J Biol Chem 279: 34938–34947.
26. Crompton MR, Bartlett TJ, MacGregor AD, Manfioletti G, Buratti E, et al. (1992) Identification of a novel vertebrate homeobox gene expressed in haematopoietic cells. Nucleic Acids Res 20: 5661–5667.
27. Morrison GM, Oikonomopoulou I, Migueles RP, Soneji S, Livigni A, et al. (2008) Anterior definitive endoderm from ESCs reveals a role for FGF signaling. Cell Stem Cell 3: 402–415.
28. Bort R, Martinez-Barbera JP, Beddington RS, Zaret KS (2004) Hex homeobox gene-dependent tissue positioning is required for organogenesis of the ventral pancreas. Development 131: 797–806.

STEM CELLS AND DEVELOPMENT
Volume 00, Number 00, 2014

DOI: 10.1089/scd.2013.0424

ORIGINAL RESEARCH REPORT

Protein Kinase C-Induced Early Growth Response Protein-1 Binding to *SNAIL* Promoter in Epithelial–Mesenchymal Transition of Human Embryonic Stem Cells

Masaki Kinehara,[1,2] Suguru Kawamura,[1,3] Sumiyo Mimura,[1,3] Mika Suga,[1] Akiko Hamada,[1] Mari Wakabayashi,[1] Hiroki Nikawa,[3] and Miho K. Furue[1]

Epithelial–mesenchymal transition (EMT) has been thought to occur during early embryogenesis, and also the differentiation process of human embryonic stem (hES) cells. Spontaneous differentiation is sometimes observed at the peripheral of the hES cell colonies in conventional culture conditions, indicating that EMT occurs in hES cell culture. However, the triggering mechanism of EMT is not yet fully understood. The balance between self-renewal and differentiation of human pluripotent stem (hPS) cells is controlled by various signal pathways, including the fibroblast growth factor (FGF)-2. However, FGF-2 has a complex role for self-renewal of hES cells. FGF-2 activates phosphatidylinositol-3 kinase/AKT, mitogen-activated protein kinase/extracellular signal-regulated kinase-1/2 kinase, and also protein kinase C (PKC). Here, we showed that a PKC rapidly induced an early growth response protein-1 (EGR-1) in hES cells, which was followed by upregulation of EMT-related genes. Before the induction of EMT-related genes, EGR-1 was translocated into the nucleus, and then bound directly to the promoter region of *SNAIL*, which is a master regulator of EMT. *SNAIL* expression was attenuated by knockdown of *EGR-1*, but upregulated by ectopic expression of *EGR-1*. EGR-1 as the downstream signal of PKC might play a key role in EMT initiation during early differentiation of hES cells. This study would lead to a more robust understanding of the mechanisms underlying the balance between self-renewal and initiation of differentiation in hPS cells.

Introduction

THE BALANCE BETWEEN self-renewal and differentiation of human pluripotent stem (hPS) cells, including embryonic stem (hES) and induced pluripotent stem cells, is controlled by various signal pathways [1–8], including transforming growth factor-β/activin A/Nodal [9–11], sphingosine-1-phosphate/platelet-derived growth factor [12], insulin growth factor (IGF)/insulin [13], and fibroblast growth factor-2 (FGF-2) [14–17]. In particular, FGF-2 signaling appears indispensable to maintain the undifferentiated state of hPS cells [18–20]. However, FGF-2 has a complex role for self-renewal of hES cells [21]. FGF-2 activates phosphatidylinositol-3 kinase (PI3K)/AKT and mitogen-activated protein kinase/extracellular signal-regulated kinase-1/2 (ERK-1/2) kinase. The PI3K/AKT pathway plays important roles in the proliferation and survival of hPS cells [22–24]. On the other hand, the ERK-1/2 pathway has reported to have diverse roles in hPS cells, such as self-renewal, cell attachment, and cell differentiation [2,25–27]. FGF-2 also induces inactive phosphorylation of glycogen synthase kinase-3 (GSK-3) [1,3,4,28] of which function has been reported to be controversial for self-renewal of hPS cells [29,30]. Moreover, we have recently reported that FGF-2 induces protein kinase C (PKC), which leads to phosphorylation of GSK-3β [4]. An activator of PKC, phorbol 12-myristate 13-acetate (PMA) changes the sharp-edged, flat, and tightly packed colonies of hPS cells to scattered cells, indicating that PKC induces the epithelial–mesenchymal transition (EMT) in hPS cells [4]. Consistent with our findings, Thomson's group reported that activation of PKC is associated with EMT, leading the hPS cell differentiation into extraembryonic endodermal (ExEn) cells [5]. However, the downstream of the PKC pathway in regulating the EMT initiation is not yet understood.

[1]Laboratory of Stem Cell Cultures, Department of Disease Bioresources Research, National Institute of Biomedical Innovation, Ibaraki, Japan.
[2]Department of Biological Science, Graduate School of Science, Hiroshima University, Higashi-Hiroshima, Japan.
[3]Department of Oral Biology and Engineering, Integrated Health Sciences, Institute of Biomedical and Health Science, Hiroshima University, Higashi-Hiroshima, Japan.

In early embryogenesis, the EMT plays crucial roles in the differentiation of multiple tissues and organs and the formation of a body plan [31]. During the EMT process, E-cadherin is downregulated. Several transcription factors have been implicated in this repression, including SNAIL, SLUG, and TWIST1 [32–37]. Actually, in hPS cell culture, spontaneous differentiation is sometimes observed with the expression of SNAIL and VIMENTIN at the peripheral of the hPS cell colonies in conventional culture conditions, indicating that EMT occurs in hPS cell culture [38–41].

In this study, we investigated molecules involved in the cascade of PKC-induced EMT in hES cells using the minimal growth factor-defined culture medium hESF9, which includes FGF-2 as the sole growth factor to remove the effects of other growth factors on EMT [17]. The results showed that the early growth response protein-1 (EGR-1; also known as NGFI-A, KROX-24, ZIF268, or TIS8) was induced by a PKC activator, PMA, and bound to the regulatory region of *SNAIL*, resulting in the upregulation of *SNAIL* and EMT-related genes. PMA-induced *SNAIL* expression was attenuated by knockdown of *EGR-1*, whereas ectopic expression of *EGR-1* induced EMT-related genes expression. These results indicated that a downstream effector of PKC signaling, EGR-1, contributed to the induction of EMT in hES cell differentiation. This study would lead to a more robust understanding of the mechanisms underlying the balance between self-renewal and initiation of differentiation in hPS cells.

Materials and Methods

Cell culture

The hES cell line, H9 [19,42] (WA09, WISC Bank; WiCell Research Institute), was routinely maintained as previously described [19]. For the experiment, the cells were seeded on a six-well plate (BD Falcon) coated with bovine fibronectin (FN; Sigma; 2 μg/cm^2) in the hESF9 medium [17] consisting of the ESF basal medium (CSTI) [43] without 4-(2-hydroxyethyl)-1-piperazine-ethanesulfonic acid supplemented with L-ascorbic acid-2-phophate (Wako), 2-mercaptoethanol, 2-ethanolamine, sodium selenite, insulin, transferrin, oleic acid conjugated with bovine fatty acid-free albumin, heparan sulfate sodium salt (all from Sigma), and FGF-2 (Katayama Kagaku Kogyo Ltd.). PMA dissolved in dimethyl sulfoxide (DMSO) was added into the medium at a final concentration of 10 nM (containing a final concentration of 0.1% DMSO). The experiments using hES cells were performed following the Guidelines for utilization of hES cells of the Ministry of Education, Culture, Sports, Science and Technology of Japan with the approval by the institutional research ethics committee.

Immunocytochemistry

Immunocytochemistry was performed as previously described [4]. The image analysis was performed by IN Cell Analyzer 2000 and IN Cell Developer Toolbox software (GE Healthcare). The primary and secondary antibodies used are listed in Supplementary Table S1 (Supplementary Data are available online at www.liebertpub.com/scd).

Real-time quantitative reverse transcription–polymerase chain reaction

Real-time quantitative reverse transcription–polymerase chain reaction (qRT-PCR) and real-time quantitative PCR (qPCR) were performed based on the SYBR Green gene expression technology in a 7300 Real Time PCR System (Applied Biosystems), according to the manufacturer's instructions. Specific primers used are listed in Supplementary Table S2.

DNA microarray

DNA microarray analysis was performed using the whole human genome DNA microarray 4x44K kit (ver.2.0) and a microarray scanner G2565BA (Agilent) according to the manufacturer's instructions (Agilent). The signal intensity data produced for each of the spots were analyzed using feature extraction (Agilent) and GeneSpring GX software (Agilent).

Chromatin immunoprecipitation assay

Chromatin immunoprecipitation (ChIP) assay was performed using the ChIP-IT Express kit (Active Motif) according to the manufacturer's instructions. Chromatin was precipitated with EGR-1 antibodies (Cell Signaling Technology) or H3K9ac antibodies (MAB Institute). The immunoprecipitated DNA samples were analyzed by qPCR. The *SNAIL* promoter was amplified with the primer pairs listed in Supplementary Table S2.

Construction of EGR-1 expression vector

The *EGR-1* expression vector was constructed as follows. The EGR1-2A-eGFP fragment coding *EGR-1* (NM_001964.2), a self-cleaving 2A peptide [44], and the enhanced green fluorescent protein (eGFP) were synthesized by the GeneArt gene synthesis service (Life Technologies). The synthesized fragment was inserted into the *Xho*I and *Not*I sites of the episomal pEBmulti-Hyg plasmid (Wako Pure Chemical Industries) to create the pEGR1-2A-eGFP plasmid. To generate the peGFP control vector, the pEGR1-2A-eGFP plasmid was digested with *Xho*I and *Sal*I restriction enzymes, and the EGR1 fragment was removed from the pEGR1-2A-eGFP plasmid. The plasmids were verified by sequencing.

Transfection

Before transfection, the hES cells were incubated with ROCK inhibitor Y-27632 (10 μM) for 1 h and dissociated into single cells by a cell dissociation solution, TrypLE^{TM} Select (Life Technologies). Pellets of 1×10^6 cells were mixed with 2 μg of the EGR-1 expression plasmid (pEB-EGR1-2A-eGFP) or control plasmid (peGFP) in 100 μL of Neon R buffer solution (Life Technologies). The cell suspension was transferred to a cuvette and electroporated using a Neon Transfection system (Life Technologies) with program (voltage 1,050, width 30, and pulses 2) according to the manufacturer's protocol. The electroporated cells were plated onto a six-well plate coated with FN in the hESF9 medium supplemented with ROCK inhibitor (10 μM). The eGFP-positive cells were selected on hygromycin B (200 μg/mL) for 6 days in the hESF9 medium.

Transfections with siRNA

Transfections with siRNA targeting human *EGR-1* (SMARTpool ON-TARGETplus, L-006526-00) or non-targeting control siRNA (ON-TARGETplus Non-targeting Pool, D-001810-10) were performed using Dharmafect1 (Dharmacon) as previously described [4]. Total RNAs or proteins were extracted for analysis 72 h after the fast transfection.

Western blot analyses

Western blot analyses were performed as described previously [4]. The protein was separated by 12.5% sodium dodeyl sulfate–polyacrylamide gel electrophoresis and transferred to polyvinylidene fluoride membranes (Millipore). The membranes were reacted with primary antibodies, peroxidase-conjugated secondary antibodies, and ECL Plus reagent (GE Healthcare). Protein bands were visualized using the LAS-4000 imager (Fujifilm). The primary antibodies used are listed in the Supporting Information Table S2.

Cell imaging analysis

The images of eGFP-positive cells in culture were captured in a cell imaging system, BioStation CT (Nikon Instruments, Inc.) at 37°C 10% CO_2. The images were analyzed by a software CL-Quant (Nikon Instruments, Inc.).

Results

EMT induction of hES cells by PMA

To confirm whether a PKC activator, PMA, induces EMT in hES cells, PMA was added into the culture of H9 hES cells grown in the defined culture conditions. The colony morphology of H9 cells was changed within 24 h after PMA addition. Compared with the control (Fig. 1A[a]), the packed colonies of undifferentiated H9 hES cells came loose and flatter cells scattered out (Fig. 1A[b]). PMA addition together with the PKC inhibitor GFX did not change the colony morphology of H9 hES cells (Fig. 1A[c]). The scattered cells were positive for SSEA-1 and VIMENTIN, and negative for NANOG or E-cadherin, and vice versa for the cells treated with PMA together with GFX (Fig. 1A[d–i]). These results indicated that the activation of PKC induced the EMT process.

To determine whether PMA promotes the expression of EMT-related genes or lineage-specific cell differentiation-associated genes, H9 hES cells were cultured in the presence of PMA with or without GFX for 48 h, and then for 4 more days after changing to a fresh medium without PMA or GFX (Supplementary Fig. S1A). qRT-PCR analysis showed that the expression of *SNAIL* rapidly increased 3 h after PMA treatment (Fig. 1B). After the *SNAIL* expression, the expression of *SLUG*, *VIMENTIN*, *FOXC2*, and *TWIST* significantly increased in a time-dependent manner in the cells treated with PMA. After the gene expression, the expression of an ExEn marker gene *SOX7* and endoderm marker genes *SOX17*, *EOMES*, *GATA4*, and *GATA6* was significantly increased in the cells (Supplementary Fig. S1B, C). On the contrary, the expression of a primitive streak marker gene *GSC* (Supplementary Fig. S1C) or ectoderm genes *MSI1*, *SOX9*, *MAP2*, *Nestin*, and *PAX3* was not induced by PMA (Supplementary Fig. S1D). PMA addition together with GFX did not change the expression profile of EMT-related genes or cell differentiation marker genes. These results confirmed that the activation of PKC induced EMT-related genes and led to ExEn differentiation.

The expression of EGR-1

To determine PKC downstream molecules involved in the EMT initiation, differences in gene expression profiles among the cells treated with DMSO (control), PMA, or PMA together with GFX were analyzed by using DNA microarrays (Fig. 2A, B). The cells were treated with PMA for 1 h, in which time period, the *SNAIL* expression was before increase as shown in Fig. 1B. We previously reported that GFX, which is a selective inhibitor of PKC-α, β, γ, δ, and ζ negated PMA-induced differentiation of hPS cells, whereas Gö6976, which is a selective inhibitor of PKC-α, β, and γ isoforms could not counteract the effect of PMA [4]. Therefore, among genes influenced by PMA (fold change ≥5.0), genes of which expression were different between the cells treated PMA or together with GFX (fold change ≥5.0) were considered to be involved in EMT (Fig. 2C). Accordingly, the analysis nominated 26 activated genes and 2 repressed genes as the candidates for PKC downstream genes (Supplementary Table S3). Among them, we found that a zinc finger transcription factor *EGR* gene family members, *EGR-1*, *EGR-2*, *EGR-3*, and *EGR-4* were increased in the PMA-treated cells. The expression levels of *EGR-1* were significantly higher in the *EGR* gene family members (Fig. 2D). Therefore, we focused on *EGR-1*, which is reported to be involved in the EMT process in epithelial cells [45,46].

To confirm the expression of *EGR-1* in the cells treated with PMA, immunocytochemistry analysis was performed using the anti-EGR-1 antibody (Fig. 2E). The result indicated EGR-1 protein expression in the cells 1 h after PMA treatment and accumulation of EGR-1 in the nucleus. EGR-1 protein expression was at low levels in the cells treated with PMA together with GFX. From these results, it was confirmed that EGR-1 expression was induced by PMA in hES cells.

Relation between EGR-1 and SNAIL

To investigate the induced expression level of EGR-1 in the cells treated with PMA, qRT-PCR analysis was performed. The results showed that the *EGR-1* expression peaked at 1 h after PMA treatment (Fig. 3A) and the induction of *SNAIL* expression peaked at 3 h after PMA treatment (Fig. 3B).

From these data above, it was predicted that the PMA-induced *EGR-1* might directly regulate the induction of *SNAIL*. To determine the relationship between *EGR-1* and *SNAIL*, the cells were transfected with siRNA targeting *EGR-1*. When the cells were treated with PMA for 3 h, the expression of PMA-induced *EGR-1* mRNA (Fig. 3C) and its protein levels (Fig. 3D, E) were significantly reduced at 1–2 h PMA treatment time, and then *SNAIL* expression (Fig. 3F) was significantly reduced at 2 h PMA treatment time, in the cells transfected with siRNA of *EGR-1* compared with those in the cells transfected with nontarget siRNA. Then, we searched the ChIP-on-chip data for EGR-1, provided by

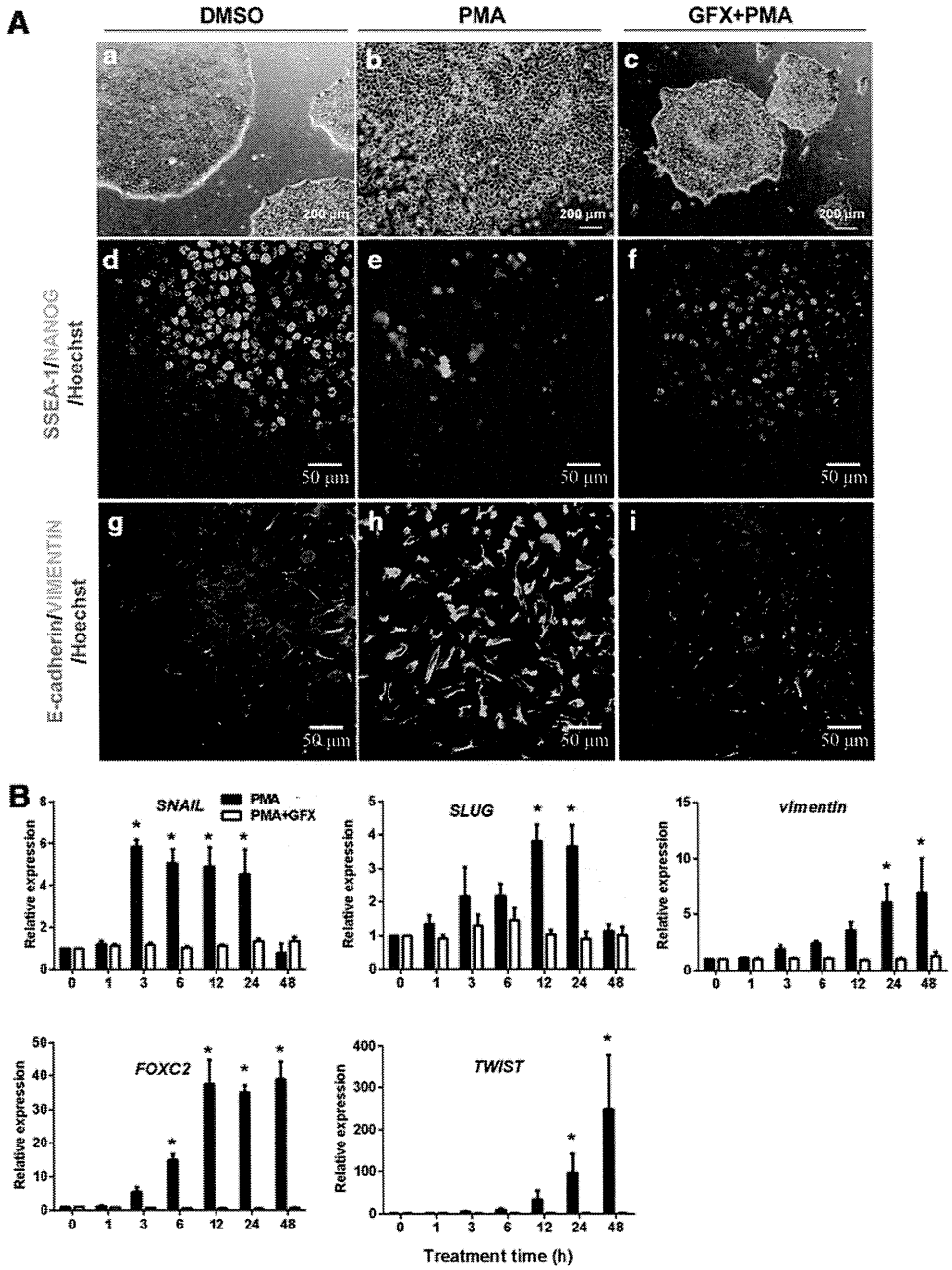

FIG. 1. Phorbol 12-myristate 13-acetate (PMA)-induced epithelial–mesenchymal transition (EMT) process in human embryonic stem (hES) cells. **(A)** Phase-contrast images and immunostaining of H9 hES cells 24 h after addition of PMA (10 nM) with or without GFX (5 μM) in the defined medium hESF9. **(a–c)** Phase-contrast images of H9 cells. **(a)** The cells in the presence of dimethyl sulfoxide (DMSO) (control). **(b)** The cells treated with PMA. **(c)** The cells treated with PMA and GFX. Scale bars = 200 μm. **(d–f)** Immunostaining for NANOG (*green*) and SSEA-1 (*red*) of the cells with DMSO **(d)**, PMA **(e)**, and PMA and GFX **(f)**. **(g–i)** Immunostaining for E-cadherin (*red*) and VIMENTIN (*green*) of the cells with DMSO **(g)**, PMA **(h)**, and PMA and GFX **(i)**. Nuclei were stained with Hoechst 33342 (*blue*). Scale bars = 50 μm. **(B)** Quantitative reverse transcription–polymerase chain reaction (qRT-PCR) analysis of the EMT-related gene expression. The cells were treated with PMA (*black bars*) or PMA in the presence of GFX (*white bars*) in the hESF9 medium for 48 h. Expression levels were all normalized against *GAPDH*. The relative expression levels of each gene were calculated from the undifferentiated H9 hES cells untreated with PMA or PMA together with GFX. The data are represented as mean ± standard error (SE, $n = 3$). $^*P < 0.05$.

the FANTOM 4 database (http://fantom.gsc.riken.jp/4/) [47]. Data showed that EGR-1 binds to the region of the *SNAIL* promoter in human THP-1 cells (Supplementary Fig. S2A). Thus, ChIP analysis was performed to determine whether EGR-1 could actually bind to the promoter region of *SNAIL*, which contains the putative EGR-1 binding site in hES H9 cells (Supplementary Fig. S2B). The result showed that EGR-1 bound to the promoter region of *SNAIL*, and that the amounts of immunoprecipitated DNA with the EGR-1 antibody was increased by PMA treatment, but decreased by

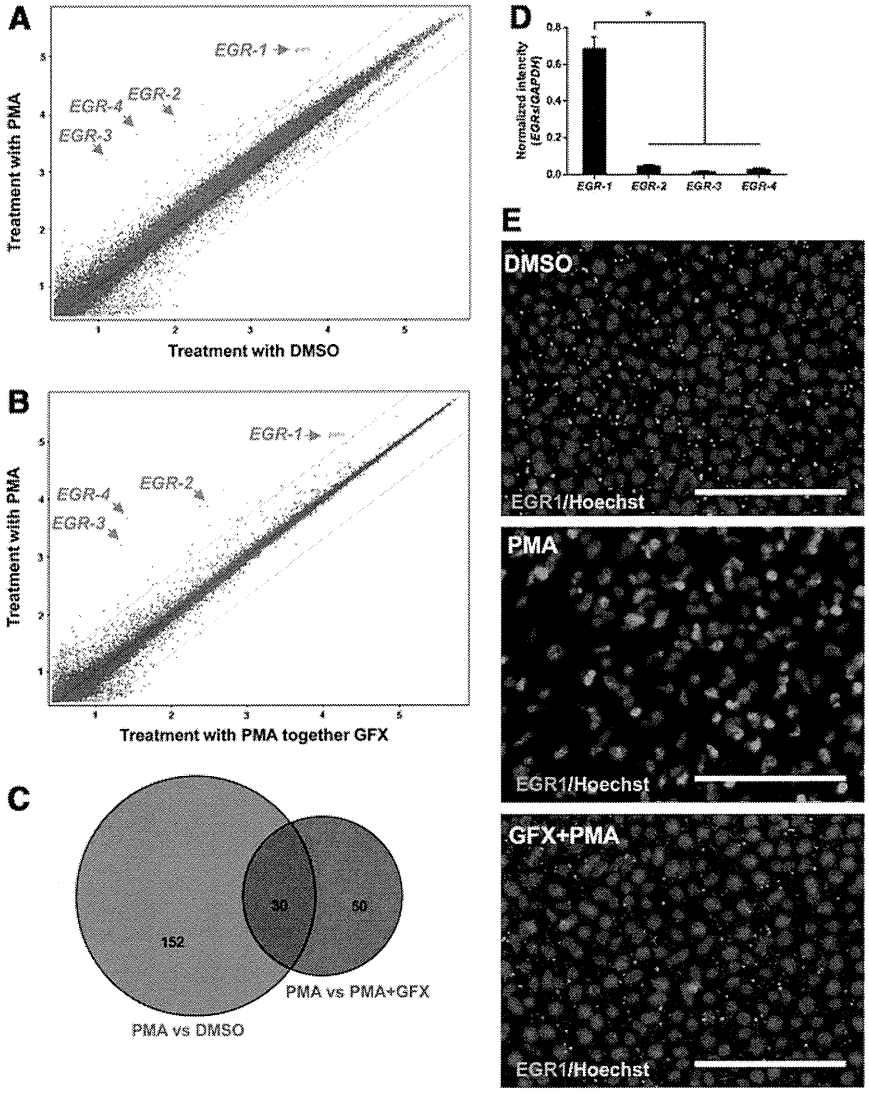

FIG. 2. Early growth response protein-1 (*EGR-1*) increases in the hES cells treated with PMA. **(A)** DNA microarray analysis of H9 hES cells treated with or without PMA for 1 h. **(B)** DNA microarray analysis of H9 hES cells treated with PMA or PMA together with GFX for 1 h. **(C)** Venn diagram of probes (*purple*) shared by the PMA-influenced probes (*red*) and GFX-influenced probes (*blue*) in DNA microarray analysis. Values in Venn diagram indicated the number of probes changed (fold change ≥ 5.0) by DNA microarray analysis at **(A)** and **(B)**. **(D)** The fluorescence intensity of each spot of *EGR* genes in the microarray was normalized against the fluorescence intensity of *GAPDH* gene. The data are represented as mean ± standard error (SE, n = 3). $^*P < 0.05$. **(E)** Immunostaining for EGR-1 (Alexa fluor 647; *red*) in H9 hES cells treated with PMA (10 nM) or PMA together with GFX (5 μM). Nuclei were stained with Hoechst 33342 (*blue*). Scale bars = 50 μm.

PMA treatment together with GFX (Fig. 3G). It is reported that EGR-1 is colocalized with histone H3 lysine 9 acetylation (H3K9ac) sites, which is tightly associated with the transcription start sites of genes [47]. Thus, H3K9ac is important for EGR-1 target site selection for gene activation. To confirm H3K9ac modification around the EGR-1 binding site in the *SNAIL* promoter, ChIP analysis was performed using the anti-H3K9ac antibody (Supplementary Fig. S2C). The result indicated that the EGR-1 binding region in the *SNAIL* promoter was colocalized with the H3K9ac site. These above results demonstrated that the PMA-induced EGR-1 was directly bound to the *SNAIL* promoter region and it resulted in the expression of *SNAIL*, suggesting that EGR-1 may play a role in EMT initiation during early differentiation of hES cells.

EMT induction by ectopic EGR-1

To confirm the function of EGR-1 as an EMT inducer in hES cells, an episomal vector carrying a CAG promoter-driven EGR1-2A-eGFP was transiently transfected into H9 cells. The expression of ectopic EGR-1 in H9 hES cells 24 h after the transfection was confirmed by western blotting analysis using the specific anti-EGR-1 antibody (Fig. 4A). The expression of *SNAIL* was significantly increased in the cells expressing ectopic EGR-1 with or without GF109203X (GFX) (Fig. 4B). Furthermore, the cells expressing ectopic EGR-1-2A-eGFP were selected on hygromycin B for 6 days, colonies became loose and scattered flatter cells. Control cell colonies maintained undifferentiated morphology (Fig. 4C). The result by qRT-PCR showed that the expression of EMT-related genes *SNAIL*, *SLUG*, and *FOXC2* were significantly upregulated in the cells expressing ectopic EGR-1, but the expression of *E-cadherin* was significantly downregulated (Fig. 4D). These results indicated that the expression of EGR-1 induced EMT in hES cells.

Discussion

In this study, we showed that PMA rapidly induced the expression of EGR-1 and accumulation of EGR-1 into the nucleus, which resulted in the expression of *SNAIL* in hES cells. PMA-induced *SNAIL* expression was attenuated by knockdown of *EGR-1*, whereas ectopic *EGR-1* expression induced EMT-related genes expression, resulting in the

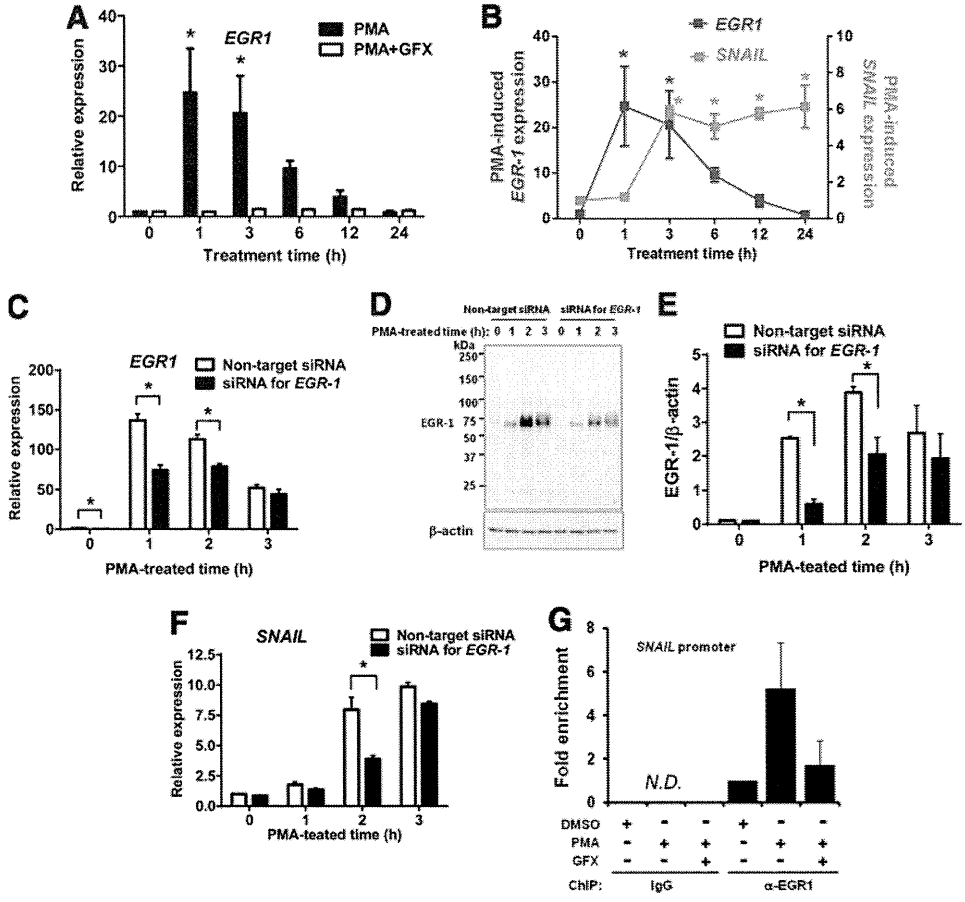

FIG. 3. PMA-induced *EGR-1* expression in hES cells. **(A)** qRT-PCR analysis of *EGR-1* expression in the cells treated with PMA (*black bars*) or PMA together with GFX (*white bars*) for 24 h. **(B)** qRT-PCR analysis of *EGR-1* (*black square*) or *SNAIL* (*gray square*) expression in the cells treated with PMA for 24 h. Expression levels were all normalized against *GAPDH*. The relative expression levels of each gene were calculated from the undifferentiated H9 hES cells untreated with PMA or PMA together with GFX. The data are represented as mean ± SE ($n = 3$). *$P < 0.05$. **(C)** qRT-PCR analysis of PMA-induced *EGR-1* expression in the cells transfected with siRNA targeting *EGR-1* (*black bars*) or nontarget control (*white bars*). Cells were treated with PMA for 3 h. Expression levels were all normalized against *GAPDH*. The relative expression levels of *EGR-1* were calculated from the nontarget siRNA-transfected H9 hES cells. The data are represented as mean ± SE ($n = 3$). *$P < 0.05$. **(D)** Western blot analysis of PMA-induced EGR-1 expression in the cells transfected with siRNA targeting *EGR-1* or nontarget control. Cells were treated with PMA for 3 h. **(E)** Quantification of the western blot result at **(D)**. Cells were transfected with siRNA targeting *EGR-1* (*black bars*) or nontarget control (*white bars*). The data are represented as mean ± SE ($n = 3$). *$P < 0.05$. **(F)** qRT-PCR analysis of PMA-induced *SNAIL* expression in the cells transfected with siRNA targeting *EGR-1* (*black bars*) or nontarget control (*white bars*). Cells were treated with PMA for 3 h. Expression levels were all normalized against *GAPDH*. The relative expression levels of *SNAIL* were calculated from the nontarget siRNA-transfected H9 hES cells. The data are represented as mean ± SE ($n = 3$). *$P < 0.05$. **(G)** Chromatin immunoprecipitation (ChIP) assay. The cells were treated with PMA (10 nM) or PMA together with GFX (5 μM) for 1 h. N.D., not detected.

induction of the EMT process in hES cells. Furthermore, EGR-1 may function in hES-specific lineage cell differentiation. The ChIP-on-ChIP database of EGR-1, provided by the FANTOM 4 database (http://fantom.gsc.riken.jp/4/) [47], showed that EGR-1 binds not only to the region of *SNAIL* promoter, but also to the promoter and intragenic regions of a number of genes. For example, EGR-1 binding sites are present in the promoter region of EMT-related genes; *E-cadherin*, *TWIST*, *VIMENTIN*, and *MMP2*, and extraembryonic and/or definitive endodermal cell lineage-associated genes; *EOMES*, *GATA6*, *SOX7*, *FOXA2*, and *CXCR4* in human THP-1 cells (Supplementary Fig. S3). These findings are consistent with our results that PMA induced EMT and also cell differentiation into the extra-embryonic endoderm in hPS cells.

The previous study reported that the SNAIL protein is phosphorylated by GSK-3β, and then the phosphorylated SNAIL protein binds to the promoter region of E-cadherin and downregulates the transcript of *E-cadherin*, leading to the EMT process [48]. These findings implied that the function of SNAIL protein induced by EGR-1 might be regulated by GSK-3β in the nucleus [48]. Although GSK-3β is generally considered to be a cytoplasmic protein, previous reports suggest that GSK-3β also functions in the nucleus [49–51]. It means that Wnt signaling promotes EMT in hPS cells. We have previously reported that phosphorylation of

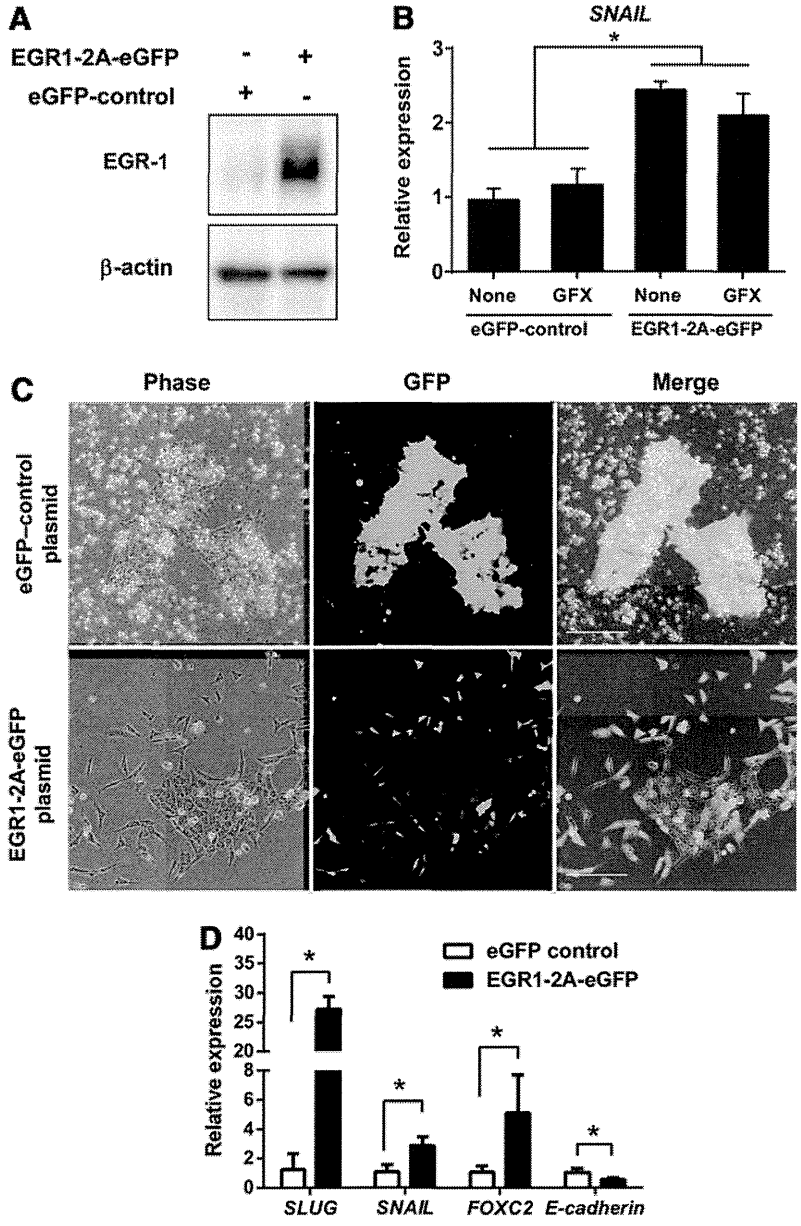

FIG. 4. EMT-related gene expression by ectopic EGR-1. **(A)** Western blot analysis of ectopic EGR-1 expression in the cells transfected with EGR1-2A-eGFP or with enhanced green fluorescent protein (eGFP) control plasmid. Transiently ectopic EGR-1 expression was confirmed by the specific EGR-1 antibody at 24 h after transfection. **(B)** qRT-PCR analysis of *SNAIL* in the cells expressing EGR1-2A-eGFP or eGFP alone in the presence or absence of GFX. Expression levels of the *SNAIL* gene were all normalized against *GAPDH*. The data are represented as mean ± SE ($n=3$). $^*P<0.05$. **(C)** Phase-contrast and fluorescence images of H9 hES cells transfected with pEGR1-2A-eGFP or peGFP control plasmid. The EGR1-2A-eGFP or eGFP alone expressing cells were selected on hygromycin B (200 μg/mL) in the hESF9 medium for 6 days. Scale bars = 200 μm. **(D)** qRT-PCR analysis of the EMT-related genes. Expression levels of genes in the cells expressing EGR1-2A-eGFP (*black bars*) or eGFP alone (*white bars*) were all normalized against *GAPDH*. The data are represented as mean ± SE ($n=3$). $^*P<0.05$.

GSK-3β is induced by FGF-2-activated PKC and that this process might be related to hPS cell differentiation [4]. This is consistent with previous studies that canonical Wnt signaling does not appear to promote stem cell maintenance [52,53]. However, this conclusion contradicts the findings of previous studies, which demonstrated that canonical Wnt signaling supports self-renewal of stem cells [6,38]. A recent study has shown the dual function of Wnt signaling in hES cells, suggesting that the pathways of self-renewal or differentiation are dependent on the presence of hES cell supporting factors [7,30,54,55]. From these studies, GSK-3 has emerged as an important regulator of undifferentiated state in hPS cells.

GSK-3β has been reported to be controlled by various growth factors, including insulin, IGF, FGF-2, and WNT3A [4,22,29,56,57]. We reported that in hPS cells, FGF-2-induced GSK-3β phosphorylation is inhibited in the presence of the PKC inhibitor, resulting in the inhibition of the PKC/GSK-3β signaling pathway to support the maintenance of an undifferentiated state [4]. From the findings above, it is implied that FGF-2 induces the expression of EGR-1 through the PKC signaling pathway, EGR-1 induced the SNAIL protein, and then PKC/GSK-3β activates SNAIL, leading to the EMT process [48] (Fig. 5). However, if FGF-2 continues to amplify the EMT process, hPS cells should rapidly differentiate. Inhibitory signaling related to the dual function of GSK-3β might exist in hPS cell culture and it can balance the FGF-2-induced EMT process to maintain the undifferentiated state although the PKC inhibitor can artificially stabilize the balance between undifferentiated state and cell differentiation. Further investigation of mechanisms involved in the regulation of PKC/EGR1/SNAIL and PKC/GSK-3β activity should be performed in future.

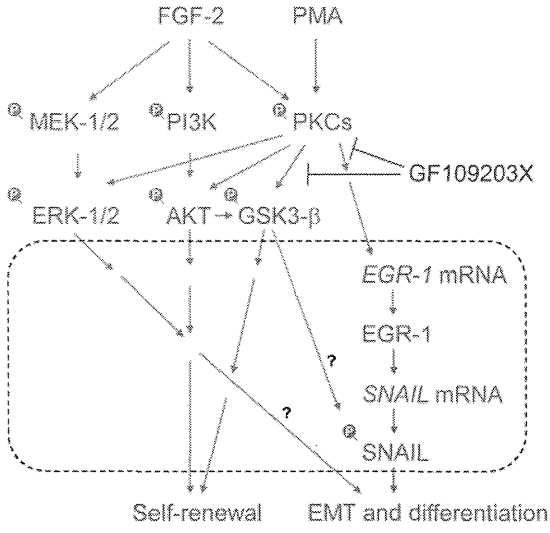

FIG. 5. A model of EMT-triggering pathways using protein kinase C (PKC) in fibroblast growth factor (FGF-2) signaling. PMA induces PKCs, and then induces EGR-1. EGR-1 directly induces the expression of *SNAIL* mRNA, leading to the EMT process [48]. GF109203X, a selective inhibitor of PKCs, negated the PKC-induced *EGR-1/SNAIL* expression, EMT process, and differentiation of human pluripotent stem cells. PKC-EGR-1-SNAIL pathways promote EMT and cell differentiation. *Dot line box* indicates the process in the nucleus.

This study clarified that PKC activation induced the EMT process through the EGR-1/SNAIL pathway suggesting that EGR-1 plays a role in the differentiation of hES cells. This finding would lead to a better understanding of the precise mechanism regulating the balance between undifferentiated state and cell differentiation in hPS cells.

Acknowledgments

This study was supported by grants-in-aid from the Ministry of Health, Labor and Welfare of Japan to M.K.F., the Ministry of Education, Culture, Sports, Science and Technology of Japan to M.K.F. and M.K., and the New Energy and Industrial Technology Development Organization (NEDO) of Japan to M.K.F. We thank Hiroko Matsumura, Ayaka Fujiki, Naoko Ueda, Yujung Liu, Daiki Tateyama, and Minako Okamura for excellent technical support, and Takayuki Fukuda and Kana Yanagihara for technical support and discussion.

Author Disclosure Statement

All the authors have read and approved the article, and hereby declare that none of them has any competing interest.

References

1. Dreesen O and AH Brivanlou. (2007). Signaling pathways in cancer and embryonic stem cells. Stem Cell Rev 3:7–17.
2. Na J, MK Furue and PW Andrews. (2010). Inhibition of ERK1/2 prevents neural and mesendodermal differentiation and promotes human embryonic stem cell self-renewal. Stem Cell Res 5:157–169.
3. Armstrong L, O Hughes, S Yung, L Hyslop, R Stewart, I Wappler, H Peters, T Walter, P Stojkovic, et al. (2006). The role of PI3K/AKT, MAPK/ERK and NFκβ signalling in the maintenance of human embryonic stem cell pluripotency and viability highlighted by transcriptional profiling and functional analysis. Hum Mol Genet 15:1894–1913.
4. Kinehara M, S Kawamura, D Tateyama, M Suga, H Matsumura, S Mimura, N Hirayama, M Hirata, K Uchio-Yamada, et al. (2013). Protein kinase C regulates human pluripotent stem cell self-renewal. PLoS One 8:e54122.
5. Feng X, J Zhang, K Smuga-Otto, S Tian, J Yu, R Stewart and JA Thomson. (2012). Protein kinase C mediated extraembryonic endoderm differentiation of human embryonic stem cells. Stem Cells 30:461–470.
6. Sato N, L Meijer, L Skaltsounis, P Greengard and AH Brivanlou. (2004). Maintenance of pluripotency in human and mouse embryonic stem cells through activation of Wnt signaling by a pharmacological GSK-3-specific inhibitor. Nat Med 10:55–63.
7. Dravid G, Z Ye, H Hammond, G Chen, A Pyle, P Donovan, X Yu and L Cheng. (2005). Defining the role of Wnt/β-catenin signaling in the survival, proliferation, and self-renewal of human embryonic stem cells. Stem Cells 23: 1489–1501.
8. Bernardo AS, T Faial, L Gardner, KK Niakan, D Ortmann, CE Senner, EM Callery, MW Trotter, M Hemberger, et al. (2011). BRACHYURY and CDX2 mediate BMP-induced differentiation of human and mouse pluripotent stem cells into embryonic and extraembryonic lineages. Cell Stem Cell 9:144–155.
9. Vallier L, D Reynolds and RA Pedersen. (2004). Nodal inhibits differentiation of human embryonic stem cells along the neuroectodermal default pathway. Dev Biol 275: 403–421.
10. Vallier L, M Alexander and RA Pedersen. (2005). Activin/nodal and FGF pathways cooperate to maintain pluripotency of human embryonic stem cells. J Cell Sci 118: 4495–4509.
11. James D, AJ Levine, D Besser and A Hemmati-Brivanlou. (2005). TGFβ/activin/nodal signaling is necessary for the maintenance of pluripotency in human embryonic stem cells. Development 132:1273–1282.
12. Pebay A, RC Wong, SM Pitson, EJ Wolvetang, GS Peh, A Filipczyk, KL Koh, I Tellis, LT Nguyen and MF Pera. (2005). Essential roles of sphingosine-1-phosphate and platelet-derived growth factor in the maintenance of human embryonic stem cells. Stem Cells 23:1541–1548.
13. Bendall SC, MH Stewart, P Menendez, D George, K Vijayaragavan, T Werbowetski-Ogilvie, V Ramos-Mejia, A Rouleau, J Yang, et al. (2007). IGF and FGF cooperatively establish the regulatory stem cell niche of pluripotent human cells *in vitro*. Nature 448:1015–1021.
14. Dvorak P, D Dvorakova, S Koskova, M Vodinska, M Najvirtova, D Krekac and A Hampl. (2005). Expression and potential role of fibroblast growth factor 2 and its receptors in human embryonic stem cells. Stem Cells 23:1200–1211.
15. Avery S, K Inniss and H Moore. (2006). The regulation of self-renewal in human embryonic stem cells. Stem Cells Dev 15:729–740.
16. Ding VM, PJ Boersema, LY Foong, C Preisinger, G Koh, S Natarajan, DY Lee, J Boekhorst, B Snel, et al. (2011). Tyrosine phosphorylation profiling in FGF-2 stimulated human embryonic stem cells. PLoS One 6:e17538.

17. Furue MK, J Na, JP Jackson, T Okamoto, M Jones, D Baker, R Hata, HD Moore, JD Sato and PW Andrews. (2008). Heparin promotes the growth of human embryonic stem cells in a defined serum-free medium. Proc Natl Acad Sci U S A 105:13409–13414.
18. Hoffman LM and MK Carpenter. (2005). Characterization and culture of human embryonic stem cells. Nat Biotechnol 23:699–708.
19. Amit M, MK Carpenter, MS Inokuma, CP Chiu, CP Harris, MA Waknitz, J Itskovitz-Eldor and JA Thomson. (2000). Clonally derived human embryonic stem cell lines maintain pluripotency and proliferative potential for prolonged periods of culture. Dev Biol 227:271–278.
20. Xu RH, RM Peck, DS Li, X Feng, T Ludwig and JA Thomson. (2005). Basic FGF and suppression of BMP signaling sustain undifferentiated proliferation of human ES cells. Nat Methods 2:185–190.
21. Eiselleova L, K Matulka, V Kriz, M Kunova, Z Schmidtova, J Neradil, B Tichy, D Dvorakova, S Pospisilova, A Hampl and P Dvorak. (2009). A complex role for FGF-2 in self-renewal, survival, and adhesion of human embryonic stem cells. Stem Cells 27:1847–1857.
22. Singh AM, D Reynolds, T Cliff, S Ohtsuka, AL Mattheyses, Y Sun, L Menendez, M Kulik and S Dalton. (2012). Signaling network crosstalk in human pluripotent cells: a Smad2/3-regulated switch that controls the balance between self-renewal and differentiation. Cell Stem Cell 10:312–326.
23. Downward J. (2004). PI 3-kinase, Akt and cell survival. Semin Cell Dev Biol 15:177–182.
24. Ohgushi M, M Matsumura, M Eiraku, K Murakami, T Aramaki, A Nishiyama, K Muguruma, T Nakano, H Suga, et al. (2010). Molecular pathway and cell state responsible for dissociation-induced apoptosis in human pluripotent stem cells. Cell Stem Cell 7:225–239.
25. Xu RH, X Chen, DS Li, R Li, GC Addicks, C Glennon, TP Zwaka and JA Thomson. (2002). BMP4 initiates human embryonic stem cell differentiation to trophoblast. Nat Biotechnol 20:1261–1264.
26. Pera MF, J Andrade, S Houssami, B Reubinoff, A Trounson, EG Stanley, D Ward-van Oostwaard and C Mummery. (2004). Regulation of human embryonic stem cell differentiation by BMP-2 and its antagonist noggin. J Cell Sci 117:1269–1280.
27. Li J, G Wang, C Wang, Y Zhao, H Zhang, Z Tan, Z Song, M Ding and H Deng. (2007). MEK/ERK signaling contributes to the maintenance of human embryonic stem cell self-renewal. Differentiation 75:299–307.
28. Schlessinger J. (2004). Common and distinct elements in cellular signaling via EGF and FGF receptors. Science 306:1506–1507.
29. Ding VM, L Ling, S Natarajan, MG Yap, SM Cool and AB Choo. (2010). FGF-2 modulates Wnt signaling in undifferentiated hESC and iPS cells through activated PI3-K/GSK3β signaling. J Cell Physiol 225:417–428.
30. Blauwkamp TA, S Nigam, R Ardehali, IL Weissman and R Nusse. (2012). Endogenous Wnt signalling in human embryonic stem cells generates an equilibrium of distinct lineage-specified progenitors. Nat Commun 3:1070.
31. Thiery JP, H Acloque, RY Huang and MA Nieto. (2009). Epithelial-mesenchymal transitions in development and disease. Cell 139:871–890.
32. Bolos V, H Peinado, MA Perez-Moreno, MF Fraga, M Esteller and A Cano. (2003). The transcription factor Slug represses *E-cadherin* expression and induces epithelial to mesenchymal transitions: a comparison with Snail and E47 repressors. J Cell Sci 116:499–511.
33. Kang Y and J Massague. (2004). Epithelial-mesenchymal transitions: twist in development and metastasis. Cell 118:277–279.
34. Comijn J, G Berx, P Vermassen, K Verschueren, L van Grunsven, E Bruyneel, M Mareel, D Huylebroeck and F van Roy. (2001). The two-handed E box binding zinc finger protein SIP1 downregulates E-cadherin and induces invasion. Mol Cell 7:1267–1278.
35. Perez-Moreno MA, A Locascio, I Rodrigo, G Dhondt, F Portillo, MA Nieto and A Cano. (2001). A new role for E12/E47 in the repression of E-cadherin expression and epithelial-mesenchymal transitions. J Biol Chem 276: 27424–27431.
36. Grooteclaes ML and SM Frisch. (2000). Evidence for a function of CtBP in epithelial gene regulation and anoikis. Oncogene 19:3823–3828.
37. Mani SA, J Yang, M Brooks, G Schwaninger, A Zhou, N Miura, JL Kutok, K Hartwell, AL Richardson and RA Weinberg. (2007). Mesenchyme Forkhead 1 (FOXC2) plays a key role in metastasis and is associated with aggressive basal-like breast cancers. Proc Natl Acad Sci U S A 104:10069–10074.
38. Ullmann U, C Gilles, M De Rycke, H Van de Velde, K Sermon and I Liebaers. (2008). GSK-3-specific inhibitor-supplemented hESC medium prevents the epithelial-mesenchymal transition process and the up-regulation of matrix metalloproteinases in hESCs cultured in feeder-free conditions. Mol Hum Reprod 14:169–179.
39. Ullmann U, P In't Veld, C Gilles, K Sermon, M De Rycke, H Van de Velde, A Van Steirteghem and I Liebaers. (2007). Epithelial-mesenchymal transition process in human embryonic stem cells cultured in feeder-free conditions. Mol Hum Reprod 13:21–32.
40. Van Hoof D, SR Braam, W Dormeyer, D Ward-van Oostwaard, AJ Heck, J Krijgsveld and CL Mummery. (2008). Feeder-free monolayer cultures of human embryonic stem cells express an epithelial plasma membrane protein profile. Stem Cells 26:2777–2781.
41. Eastham AM, H Spencer, F Soncin, S Ritson, CL Merry, PL Stern and CM Ward. (2007). Epithelial-mesenchymal transition events during human embryonic stem cell differentiation. Cancer Res 67:11254–11262.
42. Thomson JA, J Itskovitz-Eldor, SS Shapiro, MA Waknitz, JJ Swiergiel, VS Marshall and JM Jones. (1998). Embryonic stem cell lines derived from human blastocysts. Science 282:1145–1147.
43. Furue M, T Okamoto, Y Hayashi, H Okochi, M Fujimoto, Y Myoishi, T Abe, K Ohnuma, GH Sato, M Asashima and JD Sato. (2005). Leukemia inhibitory factor as an anti-apoptotic mitogen for pluripotent mouse embryonic stem cells in a serum-free medium without feeder cells. In Vitro Cell Dev Biol Anim 41:19–28.
44. Kim JH, SR Lee, LH Li, HJ Park, JH Park, KY Lee, MK Kim, BA Shin and SY Choi. (2011). High cleavage efficiency of a 2A peptide derived from porcine teschovirus-1 in human cell lines, zebrafish and mice. PLoS One 6:e18556.
45. Grotegut S, D von Schweinitz, G Christofori and F Lehembre. (2006). Hepatocyte growth factor induces cell scattering through MAPK/Egr-1-mediated upregulation of Snail. EMBO J 25:3534–3545.

46. Kuo PL, YH Chen, TC Chen, KH Shen and YL Hsu. (2011). CXCL5/ENA78 increased cell migration and epithelial-to-mesenchymal transition of hormone-independent prostate cancer by early growth response-1/snail signaling pathway. J Cell Physiol 226:1224–1231.
47. Kubosaki A, Y Tomaru, M Tagami, E Arner, H Miura, T Suzuki, M Suzuki, H Suzuki and Y Hayashizaki. (2009). Genome-wide investigation of *in vivo* EGR-1 binding sites in monocytic differentiation. Genome Biol 10:R41.
48. Zhou BP, J Deng, W Xia, J Xu, YM Li, M Gunduz and MC Hung. (2004). Dual regulation of Snail by GSK-3β-mediated phosphorylation in control of epithelial-mesenchymal transition. Nat Cell Biol 6:931–940.
49. Bechard M and S Dalton. (2009). Subcellular localization of glycogen synthase kinase 3β controls embryonic stem cell self-renewal. Mol Cell Biol 29:2092–2104.
50. Bechard M, R Trost, AM Singh and S Dalton. (2012). Frat is a phosphatidylinositol 3-kinase/Akt-regulated determinant of glycogen synthase kinase 3β subcellular localization in pluripotent cells. Mol Cell Biol 32:288–296.
51. Singh AM, M Bechard, K Smith and S Dalton. (2012). Reconciling the different roles of Gsk3β in "naive" and "primed" pluripotent stem cells. Cell Cycle 11:2991–2996.
52. Davidson KC, AM Adams, JM Goodson, CE McDonald, JC Potter, JD Berndt, TL Biechele, RJ Taylor and RT Moon. (2012). Wnt/β-catenin signaling promotes differentiation, not self-renewal, of human embryonic stem cells and is repressed by Oct4. Proc Natl Acad Sci U S A 109: 4485–4490.
53. Sumi T, N Tsuneyoshi, N Nakatsuji and H Suemori. (2008). Defining early lineage specification of human embryonic stem cells by the orchestrated balance of canonical Wnt/β-catenin, Activin/Nodal and BMP signaling. Development 135:2969–2979.
54. Cai L, Z Ye, BY Zhou, P Mali, C Zhou and L Cheng. (2007). Promoting human embryonic stem cell renewal or differentiation by modulating Wnt signal and culture conditions. Cell Res 17:62–72.
55. Villa-Diaz LG, C Pacut, NA Slawny, J Ding, KS O'Shea and GD Smith. (2009). Analysis of the factors that limit the ability of feeder cells to maintain the undifferentiated state of human embryonic stem cells. Stem Cells Dev 18: 641–651.
56. Kaidanovich-Beilin O and JR Woodgett. (2011). GSK-3: functional insights from cell biology and animal models. Front Mol Neurosci 4:40.
57. Cohen P and S Frame. (2001). The renaissance of GSK3. Nat Rev Mol Cell Biol 2:769–776.

Address correspondence to:
Dr. Miho K. Furue
Laboratory of Stem Cell Cultures
Department of Disease Bioresources Research
National Institute of Biomedical Innovation
7-6-8 Saito-Asagi
Ibaraki, Osaka 567-0085
Japan

E-mail: mkfurue@nibio.go.jp

Received for publication September 4, 2013
Accepted after revision January 10, 2014
Prepublished on Liebert Instant Online XXXX XX, XXXX

© 2014. Published by The Company of Biologists Ltd | Development (2014) 141, 91-100 doi:10.1242/dev.103168

RESEARCH ARTICLE

STEM CELLS AND REGENERATION

CCAAT/enhancer binding protein-mediated regulation of TGFβ receptor 2 expression determines the hepatoblast fate decision

Kazuo Takayama[1,2,3], Kenji Kawabata[4], Yasuhito Nagamoto[1,2], Mitsuru Inamura[1], Kazuo Ohashi[5], Hiroko Okuno[1], Tomoko Yamaguchi[4], Katsuhisa Tashiro[4], Fuminori Sakurai[1], Takao Hayakawa[6], Teruo Okano[5], Miho Kusada Furue[7,8] and Hiroyuki Mizuguchi[1,2,3,9,*]

ABSTRACT

Human embryonic stem cells (hESCs) and their derivatives are expected to be used in drug discovery, regenerative medicine and the study of human embryogenesis. Because hepatocyte differentiation from hESCs has the potential to recapitulate human liver development *in vivo*, we employed this differentiation method to investigate the molecular mechanisms underlying human hepatocyte differentiation. A previous study has shown that a gradient of transforming growth factor beta (TGFβ) signaling is required to segregate hepatocyte and cholangiocyte lineages from hepatoblasts. Although CCAAT/enhancer binding proteins (c/EBPs) are known to be important transcription factors in liver development, the relationship between TGFβ signaling and c/EBP-mediated transcriptional regulation in the hepatoblast fate decision is not well known. To clarify this relationship, we examined whether c/EBPs could determine the hepatoblast fate decision via regulation of TGFβ receptor 2 (TGFBR2) expression in the hepatoblast-like cells differentiated from hESCs. We found that *TGFBR2* promoter activity was negatively regulated by c/EBPα and positively regulated by c/EBPβ. Moreover, c/EBPα overexpression could promote hepatocyte differentiation by suppressing TGFBR2 expression, whereas c/EBPβ overexpression could promote cholangiocyte differentiation by enhancing TGFBR2 expression. Our findings demonstrated that c/EBPα and c/EBPβ determine the lineage commitment of hepatoblasts by negatively and positively regulating the expression of a common target gene, *TGFBR2*, respectively.

KEY WORDS: Hepatoblasts, c/EBP, CEBP, Human ESCs

INTRODUCTION

Many animal models, such as chick, *Xenopus*, zebrafish and mouse, have been used to investigate the molecular mechanisms of liver development. Because many functions of the key molecules in liver development are conserved in these species, studies on liver development in these animals can be highly informative with respect that in humans. However, some functions of important molecules in liver development might differ between human and other species. Although analysis using genetically modified mice has been successfully performed, it is not of course possible to perform genetic experiments to elucidate molecular mechanisms of liver development in human. Pluripotent stem cells, such as human embryonic stem cells (hESCs), are expected to overcome some of these problems in the study of human embryogenesis, including liver development, because the gene expression profiles of this model are similar to those in normal liver development (Agarwal et al., 2008; DeLaForest et al., 2011).

During liver development, hepatoblasts differentiate into hepatocytes and cholangiocytes. A previous study has shown that a high concentration of transforming growth factor beta (TGFβ) could give rise to cholangiocyte differentiation from hepatoblasts (Clotman et al., 2005). To transmit the TGFβ signaling, TGFβ receptor 2 (TGFBR2) has to be stimulated by TGFβ1, TGFβ2 or TGFβ3 (Kitisin et al., 2007). TGFβ binding to the extracellular domain of TGFBR2 induces a conformational change, resulting in the phosphorylation and activation of TGFBR1. TGFBR1 phosphorylates SMAD2 or SMAD3, which binds to SMAD4, and then the SMAD complexes move into the nucleus and function as transcription factors to express various kinds of differentiation-related genes (Kitisin et al., 2007). Although the function of TGFBR2 in regeneration of the adult liver has been thoroughly examined (Oe et al., 2004), the function of TGFBR2 in the hepatoblast fate decision has not been elucidated.

CCAAT/enhancer binding protein (c/EBP) transcription factors play decisive roles in the differentiation of various cell types, including hepatocytes (Tomizawa et al., 1998; Yamasaki et al., 2006). The analysis of *c/EBPα* (*Cebpa*) knockout mice has shown that many abnormal pseudoglandular structures, which co-express antigens specific for both hepatocytes and cholangiocytes, are present in the liver parenchyma (Tomizawa et al., 1998). These data demonstrated that c/EBPα plays an important role in hepatocyte differentiation. It is also known that the suppression of c/EBPα expression in periportal hepatoblasts stimulates cholangiocyte differentiation (Yamasaki et al., 2006). Although the function of c/EBPα in liver development is well known, the relationship between TGFβ signaling and c/EBPα-mediated transcriptional regulation in the hepatoblast fate decision is poorly understood. c/EBPβ is also known to be an important factor for liver function (Chen et al., 2000), although the function of c/EBPβ in the cell fate decision of hepatoblasts is not well known. c/EBPα and c/EBPβ bind to the same DNA binding site. However, the promoter activity of hepatocyte-specific genes, such as those encoding hepatocyte nuclear factor 6 (HNF6, also known as ONECUT1) and UGT2B1,

[1]Laboratory of Biochemistry and Molecular Biology, Graduate School of Pharmaceutical Sciences, Osaka University, Osaka 565-0871, Japan. [2]Laboratory of Hepatocyte Differentiation, National Institute of Biomedical Innovation, Osaka 567-0085, Japan. [3]iPS Cell-based Research Project on Hepatic Toxicity and Metabolism, Graduate School of Pharmaceutical Sciences, Osaka University, Osaka 565-0871, Japan. [4]Laboratory of Stem Cell Regulation, National Institute of Biomedical Innovation, Osaka 567-0085, Japan. [5]Institute of Advanced Biomedical Engineering and Science, Tokyo Women's Medical University, Tokyo 162-8666, Japan. [6]Pharmaceutical Research and Technology Institute, Kinki University, Osaka 577-8502, Japan. [7]Laboratory of Embryonic Stem Cell Cultures, Department of Disease Bioresources Research, National Institute of Biomedical Innovation, Osaka 567-0085, Japan. [8]Department of Embryonic Stem Cell Research, Field of Stem Cell Research, Institute for Frontier Medical Sciences, Kyoto University, Kyoto 606-8507, Japan. [9]The Center for Advanced Medical Engineering and Informatics, Osaka University, Osaka 565-0871, Japan.

*Author for correspondence (mizuguch@phs.osaka-u.ac.jp)

Received 27 August 2013; Accepted 3 October 2013

Development (2014) doi:10.1242/dev.103168

is positively regulated by c/EBPα but not c/EBPβ (Hansen et al., 1998; Plumb-Rudewiez et al., 2004), suggesting that the functions of c/EBPα and c/EBPβ in the hepatoblast fate decision might be different.

In the present study, we first examined the function of TGFBR2 in the hepatoblast fate decision using hESC-derived hepatoblast-like cells, which have the ability to self-replicate, differentiate into both hepatocyte and cholangiocyte lineages, and repopulate the liver of carbon tetrachloride (CCl_4)-treated immunodeficient mice. *In vitro* gain- and loss-of-function analyses and *in vivo* transplantation analysis were performed. Next, we investigated how TGFBR2 expression is regulated in the hepatoblast fate decision. Finally, we examined whether our findings could be reproduced in delta-like 1 homolog (Dlk1)-positive hepatoblasts obtained from the liver of E13.5 mice. To the best of our knowledge, this study provides the first evidence of c/EBP-mediated regulation of TGFBR2 expression in the human hepatoblast fate decision.

RESULTS

Hepatoblast-like cells are generated from hESCs

First, we investigated whether the hepatoblast-like cells (HBCs), which were differentiated from hESCs as described in supplementary material Fig. S1A, have similar characteristics to human hepatoblasts. We recently found that hESC-derived HBCs could be purified and maintained on human laminin 111 (LN111)-coated dishes (Takayama et al., 2013). The long-term cultured HBC population (HBCs passaged more than three times were used in this study) were nearly homogeneous and expressed human hepatoblast markers such as alpha-fetoprotein (AFP), albumin (ALB), cytokeratin 19 (CK19, also known as KRT19) and EPCAM (Schmelzer et al., 2007) (supplementary material Fig. S1B). In addition, most of the colonies observed on human LN111-coated plates were ALB and CK19 double positive, although a few colonies were ALB single positive, CK19 single positive, or ALB and CK19 double negative (supplementary material Fig. S1C). To examine the hepatocyte differentiation capacity of the HBCs *in vivo*, these cells were transplanted into CCl_4-treated immunodeficient mice. The hepatocyte functionality of the transplanted cells was assessed by measuring secreted human ALB levels in the recipient mice (supplementary material Fig. S1D). Human ALB serum was detected in the mice that were transplanted with the HBCs, but not in the control mice. These results demonstrated that the HBCs generated from hESCs have similar characteristics to human hepatoblasts and would therefore provide a valuable tool to investigate the mechanisms of human liver development. In the present study, HBCs generated from hESCs were used to elucidate the mechanisms of the hepatoblast fate decision.

TGFBR2 expression is decreased in hepatocyte differentiation but increased in cholangiocyte differentiation

The HBCs used in this study have the ability to differentiate into both hepatocyte-like cells [cytochrome P450 3A4 (CYP3A4) positive; Fig. 1B] and cholangiocyte-like cells (CK19 positive; Fig. 1C) (the protocols are described in Fig. 1A). Because the expression pattern of TGFBR2 during differentiation from hepatoblasts is not well known, we examined it in hepatocyte and cholangiocyte differentiation from HBCs. *TGFBR2* was downregulated during hepatocyte differentiation from HBCs (Fig. 1D), but upregulated in cholangiocyte differentiation from HBCs (Fig. 1E). After the HBCs were cultured on Matrigel, the cells were fractionated into three populations according to the level of TGFBR2 expression (TGFBR2-negative, -lo or -hi; Fig. 1F). The HBC-derived TGFBR2-lo cells strongly expressed *αAT* and *CYP3A4* (hepatocyte markers), whereas the HBC-derived TGFBR2-hi cells strongly expressed *SOX9* and integrin β4 (*ITGB4*) (cholangiocyte markers). These data suggest that the TGFBR2 expression level is decreased in hepatic differentiation, but increased in biliary differentiation of the HBCs.

The cell fate decision of HBCs is regulated by TGFβ signals

To examine the function of TGFβ1, β2 and β3 (all of which are ligands of TGFBR2) in the hepatoblast fate decision, HBCs were cultured in medium containing TGFβ1, β2 or β3 (Fig. 2A,B). The expression levels of cholangiocyte marker genes were upregulated by addition of TGFβ1 or TGFβ2, but not TGFβ3 (Fig. 2A), whereas those of hepatocyte markers were downregulated by addition of TGFβ1 or TGFβ2 (Fig. 2B). To ascertain that TGFBR2 is also important in the hepatoblast fate decision, HBCs were cultured in medium containing SB-431542, which inhibits TGFβ signaling (Fig. 2C,D). Hepatocyte marker genes were upregulated by inhibition of TGFβ signaling (Fig. 2C), whereas cholangiocyte markers were downregulated (Fig. 2D). To confirm the function of TGFβ1, β2 and β3 in the hepatoblast fate decision, colony assays of the HBCs were performed in the presence or absence of TGFβ1, β2 or β3 (Fig. 2E). The number of CK19 single-positive colonies was significantly increased in TGFβ1- or β2-treated HBCs. By contrast, the number of ALB and CK19 double-positive colonies was reduced in TGFβ1-, β2- or β3-treated HBCs. These data indicated that TGFβ1 and β2 positively regulate the biliary differentiation of HBCs. Taken together, the findings suggested that TGFBR2 might be a key molecule in the regulation of hepato-bilary lineage segregation.

TGFBR2 plays an important role in the cell fate decision of HBCs

To examine whether TGFBR2 plays an important role in the hepatoblast fate decision, *in vitro* gain- and loss-of-function analysis of TGFBR2 was performed in the HBCs. We used siRNA in knockdown experiments (supplementary material Fig. S2) during HBC differentiation on Matrigel. Whereas TGFBR2-suppressing siRNA (si-TGFBR2) transfection upregulated the expression of hepatocyte markers, it downregulated cholangiocyte markers (Fig. 3A). si-TGFBR2 transfection increased the percentage of asialoglycoprotein receptor 1 (ASGR1)-positive hepatocyte-like cells (Fig. 3B). By contrast, it decreased the percentage of aquaporin 1 (AQP1)-positive cholangiocyte-like cells. These results suggest that TGFBR2 knockdown promotes hepatocyte differentiation, whereas it inhibits cholangiocyte differentiation. Next, we used Ad vector to perform efficient transduction into the HBCs (supplementary material Fig. S3) and ascertained *TGFBR2* gene expression in TGFBR2-expressing Ad vector (Ad-TGFBR2)-transduced cells (supplementary material Fig. S4). Ad-TGFBR2 transduction downregulated the expression of hepatocyte markers, whereas it upregulated cholangiocyte markers (Fig. 3C). Ad-TGFBR2 transduction decreased the percentage of ASGR1-positive hepatocyte-like cells but increased the percentage of AQP1-positive cholangiocyte-like cells (Fig. 3D). These results suggest that TGFBR2 overexpression inhibits hepatocyte differentiation, whereas it promotes cholangiocyte differentiation. Taken together, these results suggest that TGFBR2 plays an important role in deciding the differentiation lineage of HBCs.

To investigate whether hepatoblasts would undergo differentiation in a TGFBR2-associated manner *in vivo*, HBCs transfected/transduced with si-control, si-TGFBR2, Ad-LacZ or Ad-

Development (2014) doi:10.1242/dev.103168

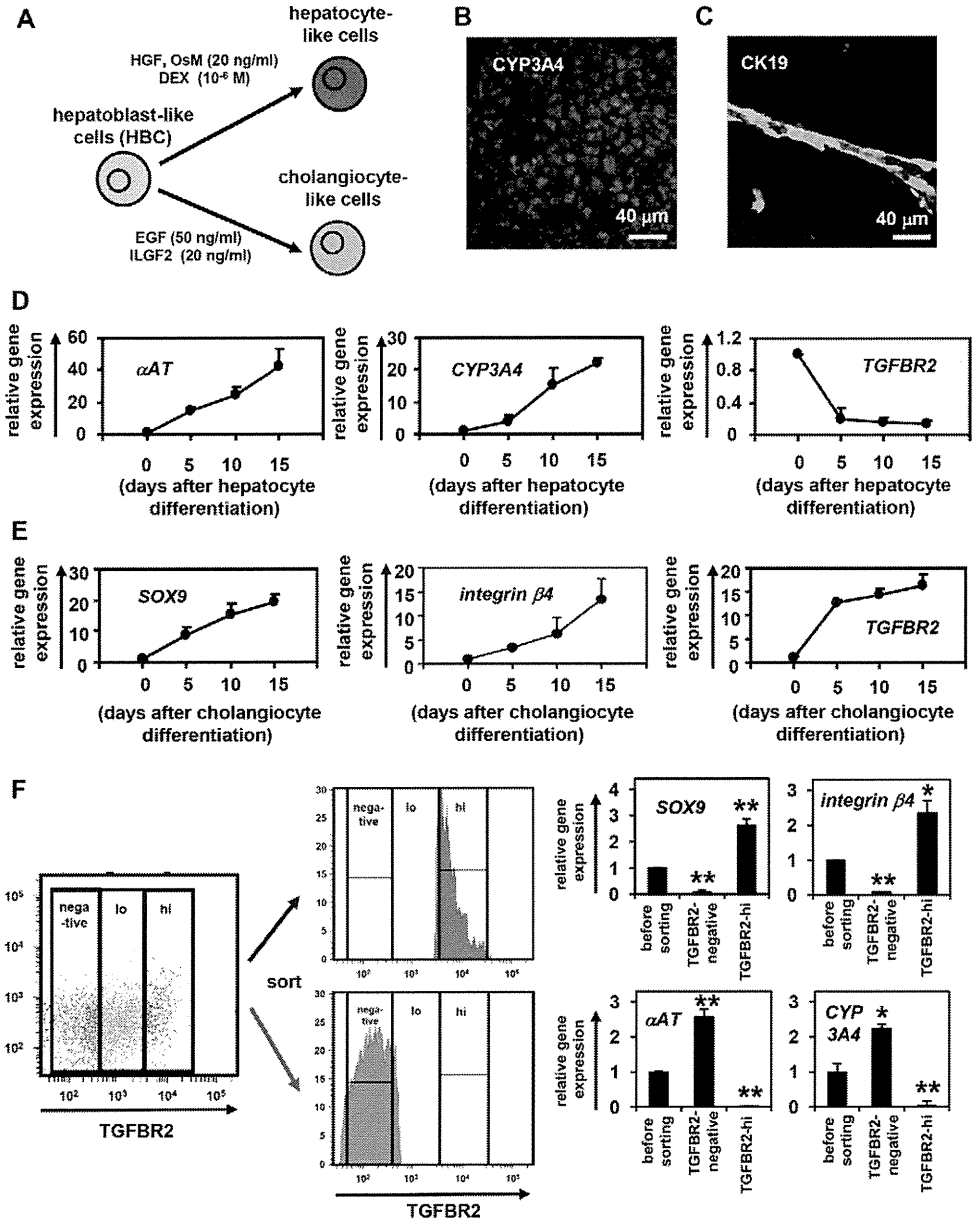

Fig. 1. HBCs can differentiate into both hepatocyte and cholangiocyte lineages. (A) The strategy for hepatocyte and cholangiocyte differentiation from HBCs. (B,C) The HBC-derived hepatocyte-like cells or cholangiocyte-like cells were subjected to immunostaining with anti-CYP3A4 (red, B) or anti-CK19 (green, C) antibodies, respectively. (D,E) Temporal gene expression levels of hepatocyte markers (*αAT* and *CYP3A4*) (D) or cholangiocyte markers (*SOX9* and integrin β4) (E) during hepatocyte or cholangiocyte differentiation as measured by real-time RT-PCR. The temporal gene expression of *TGFBR2* was also examined. The gene expression levels in HBCs were taken as 1.0. (F) HBCs were cultured on Matrigel for 5 days, and then the expression level of TGFBR2 was examined by FACS analysis. TGFBR2-negative, -lo and -hi populations were collected and real-time RT-PCR analysis was performed to measure the expression levels of hepatocyte markers (*αAT* and *CYP3A4*) and cholangiocyte markers (*SOX9* and integrin β4). **P*<0.05, ***P*<0.01 (compared with 'before sorting'). Error bars indicate s.d. Statistical analysis was performed using the unpaired two-tailed Student's *t*-test (*n*=3).

TGFBR2 were transplanted into CCl_4-treated immunodeficient mice (Fig. 3E,F). Although some of the si-control-transfected or Ad-LacZ-transduced HBCs remained as HBCs (HNF4α and CK19 double positive), most of them showed *in vitro* differentiation toward hepatocyte-like cells (HNF4α single positive) (Fig. 3E, top row). By contrast, Ad-TGFBR2-transduced HBCs were predominantly committed to cholangiocyte-like cells (CK19 single positive) and si-TGFBR2-transfected HBCs were predominantly committed to hepatocyte-like cells (HNF4α single positive) (Fig. 3E, bottom row). Ad-TGFBR2 transduction decreased the percentage of HNF4α-positive hepatocyte-like cells, whereas it increased the percentage of CK19-positive cholangiocyte-like cells (supplementary material Fig. S5). The hepatocyte functionality of the *in vivo* differentiated HBCs was assessed by measuring secreted human ALB levels in the recipient mice (Fig. 3F). Mice that were transplanted with Ad-TGFBR2-transduced HBCs showed lower human ALB serum levels than those transplanted with Ad-LacZ-transduced HBCs, and the mice that were transplanted with si-TGFBR2-transfected HBCs showed higher human ALB serum levels than those transplanted with si-control-transfected HBCs. These data suggest that cholangiocyte or hepatocyte differentiation was promoted by TGFBR2 overexpression or knockdown, respectively. Thus, based on these data from *in vitro* and *in vivo* experiments, TGFBR2 plays an important role in deciding the differentiation lineage of HBCs.

TGFBR2 promoter activity and expression are negatively regulated by c/EBPα and positively regulated by c/EBPβ

A previous study has shown that TGFBR2 expression is upregulated in *Hnf6* knockout mice (Clotman et al., 2005), although we confirmed by ChIP assay that HNF6 does not bind to the *TGFBR2* promoter region (data not shown). Because c/EBPα is important in the hepatoblast fate decision (Suzuki et al., 2003), we expected that c/EBPs might directly regulate TGFBR2 expression. The *TGFBR2* promoter region was analyzed to examine whether TGFBR2 expression is regulated by c/EBPs. Some c/EBP binding sites (supplementary material Fig. S6) were predicted by rVista 2.0 (http://rvista.dcode.org/) (Fig. 4A). By performing a ChIP assay, one